R. & M. No. 3289

MINISTRY OF AVIATION

AERONAUTICAL RESEARCH COUNCIL
REPORTS AND MEMORANDA

The Use of Conical Camber to Produce Flow Attachment at the Leading Edge of a Delta Wing and to Minimize Lift-Dependent Drag at Sonic and Supersonic Speeds

By

J. H. B. SMITH and K. W. MANGLER

LONDON : HER MAJESTY'S STATIONERY OFFICE

1963

PRICE 13*s*. 6*d*. NET

The Use of Conical Camber to Produce Flow Attachment at the Leading Edge of a Delta Wing and to Minimize Lift-Dependent Drag at Sonic and Supersonic Speeds

By

J. H. B. Smith and K. W. Mangler

Communicated by the Director-General of Scientific Research (Air),
Ministry of Supply

Summary.—In an attempt to avoid flow separation at the leading edge of a thin delta wing with subsonic leading edges, an attachment line is prescribed there. This is done by requiring the load, as predicted by attached-flow theory, to vanish along the leading edge at the design lift coefficient. For sonic speed, a complete account of this flow is given in terms of slender-wing theory and the load distributions corresponding to arbitrary conical camber are calculated. For supersonic speeds, load distributions arising in the slender-wing theory are considered and the corresponding conical-camber distributions are found by linearized theory. The lift-dependent drag for a given lift is then minimized with respect to the coefficients of a linear combination of these load distributions. It is found that the lift-dependent drag factor for these conically-cambered wings approaches the value it takes for the attached flow (in which leading-edge suction occurs) past the uncambered wing at the same Mach number, as more terms are included in the linear combination. However, when the leading edge is almost sonic an appreciable reduction is predicted. The corresponding load distributions and wing shapes are calculated and drawn. The optimum shapes for a fixed number of terms resemble flat plates drooped downwards near their leading edges, so that the localized leading-edge suction is replaced by a distributed force on a forward-facing surface, producing an effect of similar magnitude.

---

1. *Introduction.*—The linearized theory of the attached flow past a flat-plate delta wing at incidence at sonic or supersonic speeds predicts infinite values of velocity and pressure at the leading edge where this is subsonic. This singularity results in a thrust force, localized at the leading edge, which alleviates the drag as calculated from the pressure distribution over the remainder of the wing. If the leading edge is highly swept, however, the flow separates there, producing higher lift for given incidence than attached-flow theory predicts and no thrust force. These changes affect the maximum lift/drag ratio in opposite directions, but calculations based on Ref. 1 suggest that, for wings thin enough for their lifting effects to be given by flat-plate theory, the maximum lift/drag ratio is reduced below that predicted by attached-flow theory.

It seems desirable therefore to avoid leading-edge separation at the design incidence by warping (*i.e.*, cambering and twisting) the mean surface of the wing to avoid the leading-edge singularity in the pressure and velocity distributions. This is equivalent to requiring that the

---

attachment line, as defined by Maskell[2], which occurs on the under surface of the flat plate at not too high incidences, should be at the leading edge of the warped wing at the design incidence. The removal of the singularity removes the localized leading-edge suction ; but it seems reasonable to expect, on the analogy of two-dimensional aerofoil theory, that an axial force of similar strength may be achieved from the distributed suction acting on a forward-facing wing surface. Thus we may hope to obtain a theoretical value for the lift-dependent drag on a wing having leading-edge attachment similar to that given by attached-flow theory for a flat plate at the same lift.   The advantage of the warped wing will then lie in that its predicted characteristics are more likely to be realized in a real fluid, since the flow past it is more likely to stay attached.

In the present paper we restrict our consideration to conical camber, *i.e.*, camber for which the surface slope, and so the upwash, are constant along rays through the wing apex, and assume the resulting velocity field is conical.   We impose the condition of flow attachment along the leading edge by requiring the load, as calculated by attached-flow theory, to vanish there ; and then seek a minimum of the drag due to lift for prescribed lift.

The same problem of warping a wing to reduce the lift-dependent drag and maintain attached flow along the leading edge is being treated by Roper[3], without the restriction to conical camber. Her method is an extension of that of Ref. 4.   By combining solutions obtained previously, she obtains certain camber surfaces with fairly simple upwash distributions, and known load distributions which vanish along the leading edge.   These are combined in such a way as to produce low values of the lift-dependent drag, while the load at the leading edge remains zero. The values so far obtained for the lift-dependent drag lie a little closer to those for the attached flow past a flat plate (*i.e.*, are a little lower) than we have been able to achieve with conical camber.

On the other hand, the restriction to conical camber simplifies the mathematical treatment considerably.   Further, since the family of wings having the same conical distribution of surface slope contains some members which are geometrical cones, an impression of the complete flow field can be obtained with less effort than is required in the case of more complicated warped wings.   Conical camber may also have some advantage over more complicated shapes in off-design conditions ; since, at any supersonic speed, the load will vanish along the leading edge of a conically-cambered wing at some incidence.   Thus the attachment line is unlikely to lie on the upper surface for part of the span and on the lower surface for the remainder, even away from the design incidence and Mach number.

Insofar as our object is the reduction of lift-dependent drag at supersonic speeds, recent American work on wave drag due to lift is relevant.   For wings which lie near the axis of the Mach cone, it has been shown[5,6,7] that the lengthwise distribution of cross-loading* has a dominant influence on the lift-dependent wave drag.   Thus our consideration of conical fields (in which the distribution of cross-loading is linear) may be unfortunately restrictive and the approach of Ref. 3 may be more fruitful.   For these wings lying near the axis of the Mach cone the wave drag due to lift is a relatively small part of the lift-dependent drag so that deviations from the optimum are less important.   For wings with leading edges closer to the Mach cone, when the wave drag due to lift exceeds the vortex drag, the wave drag depends on the entire load distribution.

Two approaches to the design problem of warping a delta wing to reduce the lift-dependent drag have been followed.   Either the distribution of the load or the upwash is specified over the planform as a simple function involving a few parameters, and the other calculated.   The drag is then minimized with respect to the parameters.   Specification of the upwash is not well suited to the requirement of attachment at the leading edge, since the load, and so the singularity, is an outcome of the calculation (but *see* Ref. 3).   The authors (Tucker[8], Grant[9], Boyd *et al*[10],

---

* We use ' load ' for the difference of pressure between the lower and upper surfaces of the wing ; and ' loading ' for a single integral of the load.   The ' cross-loading ' is the integral of the load across the local span at a given chordwise station.

2

Tsien[11]) who have specified the load include the uniform load distribution as an element in their expressions. This leads to results which, strictly speaking, are inconsistent with linear theory, since they predict infinite surface slope at the centre-line and leading edge. The former can be removed by adding load distributions of other forms, but the latter remains, the result of trying to maintain a finite pressure difference at a subsonic edge. In certain cases this distribution may be useful, for instance when a thickness distribution is to be added ; but in calculations of the lift-dependent drag based on omitting any suction forces which may occur, or on prescribing *a priori* that none shall occur, it may exert considerable influence. This is because the favourable axial force in these cases is obtained by the action of suction peaks on forward-facing surfaces and the steeper the surface, the lower the drag factor (*see* Fig. 5, for example). Thus the results of these references depend to an unknown extent on this assumption that a finite pressure difference can be maintained at a subsonic edge. In this paper we consider only load distributions which arise in slender-wing theory from the use of analytic functions and which produce velocity distributions finite everywhere on the wing.

In Section 2 the mathematical basis of the theory is given and then the results are described and discussed in Section 3, which is intended to be comprehensible without the earlier section. The theory proceeds by building up the upwash due to a conical load distribution which vanishes at the leading edge from the upwash field of a uniformly-loaded delta wing in supersonic linearized theory. (Thus the uniform load distribution itself is excluded.) A derivative of the upwash so found is readily expressed in terms of the upwash due to the same loading at sonic speed, leading to simple expressions for the upwash and its derivative at any supersonic speed at which the leading edge is subsonic. The equation for the derivative of the upwash in terms of the load distribution is a standard integral equation for the derivative of the load distribution, whose inverse is known. Thus equations are available for the calculation of upwash from load distribution and *vice versa*. A linear combination of load distributions is considered, with their associated upwash distributions. The lift-dependent drag factor is then found as a quadratic form in the coefficients of the linear combination, and this is minimized by the method of Lagrange, using an undetermined multiplier. The results are given as graphs, discussed in Section 3, with some conclusions drawn in Section 4.

2. *The Theory of the Conically-Cambered Lifting Surface with Subsonic Leading Edges at Sonic and Supersonic Speeds.*—2.1. *The Integral Equation for Conical Velocity Fields.*—We consider an unyawed delta wing of apex angle 2γ, at a Mach number M, whose leading edges lie inside the Mach cone from the apex (Fig. 1). We consider distributions of camber and twist such that the surface slope in the streamwise direction is constant along rays through the apex (calling this conical camber) and assume that the velocity field is conical, so that the load is constant along rays through the apex. The influence of the Mach number on the flow is expressed entirely through the parameter $a = \tan \gamma / \tan \mu$, where $\mu = \operatorname{cosec}^{-1} M$ is the Mach angle and 2γ is the apex angle. We are concerned with values of a from 0 (slender-wing theory) to 1 (sonic leading edge). Introducing $\tan \gamma = K$, $\cot \mu = \sqrt{(M^2 - 1)} = \beta$, we have $a = \beta K$.

With a system of axes, origin at the apex, Ox parallel to the undisturbed flow, Oy to starboard, Oz upwards, we introduce the conical co-ordinate $\eta = y/s$, where $s = Kx$ is the local half-span. Then the load distribution is a function of η only. Considerations of the approach to the problem through conformal transformation, combined with the physical requirement that the load distribution be integrable, lead us to write it in the form

$$\frac{A}{\sqrt{(1 - \eta^2)}} + l(\eta)$$

where $l(-\eta) = l(\eta)$ and $l(1) = 0$. The first term of this is simply the load distribution on a flat plate at incidence, so we shall ignore it and restrict our analysis to symmetrical load distributions vanishing at the leading edge. Since the theory is linear, multiples of the flat-plate solution may always be superposed on those we obtain.

Such a symmetrical, conical load distribution, vanishing at the leading edge, may be regarded as made up of uniform elemental loads over triangular regions of differing apex angles (*see* Fig. 2). A constant load δl_n over a triangle $|y| < K_n x$ produces an upwash

$$\frac{\delta w_n}{V} = \frac{\delta l_n}{4\pi} \left\{ \frac{\sqrt{(1 - \beta^2 K_n^2)}}{K_n} \left(\cosh^{-1} \frac{x - \beta^2 K_n y}{\beta |y - K_n x|} + \cosh^{-1} \frac{x + \beta^2 K_n y}{\beta |y + K_n x|} \right) - \right.$$

$$\left. - \frac{2}{K_n} \cosh^{-1} \left| \frac{x}{\beta y} \right| \right\} \quad .. \quad .. \quad .. \quad .. \quad .. \quad .. \quad .. \quad .. \quad .. \quad (1)$$

in the plane $z = 0$. This is derived in the same way as equation (11-4) of Ref. 12. Writing

$$\delta w_n = \frac{dw}{d\eta'} \delta \eta' , \qquad \delta l_n = -\frac{dl}{d\eta'} \delta \eta' , \qquad K_n = K\eta' \ (0 \leqslant \eta' \leqslant 1)$$

and summing over the planform, we obtain

$$\frac{w(x, y)}{V} = -\frac{1}{4\pi} \int_0^1 \frac{dl}{d\eta'} \left\{ \frac{\sqrt{(1 - a^2\eta'^2)}}{K\eta'} \left(\cosh^{-1} \frac{x - \beta^2 K y \eta'}{\beta |y - K x \eta'|} + \cosh^{-1} \frac{x + \beta^2 K y \eta'}{\beta |y + K x \eta'|} \right) - \right.$$

$$\left. - \frac{2}{K\eta'} \cosh^{-1} \left| \frac{x}{\beta y} \right| \right\} d\eta' . \quad .. \quad .. \quad .. \quad .. \quad .. \quad .. \quad .. \quad .. \quad (2)$$

Substituting $y = \eta s = K\eta x$ and remembering that $dl/d\eta'$ is an odd function, we have

$$\frac{w(\eta)}{KV} = -\frac{1}{2\pi} \int_{-1}^1 \frac{d}{d\eta'} \left(\frac{l(\eta')}{4K^2} \right) \left\{ \sqrt{(1 - a^2\eta'^2)} \left(\cosh^{-1} \frac{1 - a^2\eta\eta'}{a|\eta - \eta'|} + \cosh^{-1} \frac{1 + a^2\eta\eta'}{a|\eta + \eta'|} \right) - \right.$$

$$\left. - 2 \cosh^{-1} \frac{1}{a|\eta|} \right\} \frac{d\eta'}{\eta'}$$

$$= -\frac{1}{\pi} \int_{-1}^1 \frac{d}{d\eta'} \left(\frac{l(\eta')}{4K^2} \right) \left\{ \sqrt{(1 - a^2\eta'^2)} \log \frac{\sqrt{(1 - a^2\eta^2)} + \sqrt{(1 - a^2\eta'^2)}}{a\sqrt{|\eta^2 - \eta'^2|}} - \right.$$

$$\left. - \log \frac{1 + \sqrt{(1 - a^2\eta^2)}}{a|\eta|} \right\} \frac{d\eta'}{\eta'} . \quad .. \quad .. \quad .. \quad .. \quad .. \quad .. \quad .. \quad (3)$$

The derivative with respect to η of the curly bracket in (3) reduces to

$$-\frac{\sqrt{(1 - a^2\eta^2)}}{\eta} \frac{\eta'^2}{\eta^2 - \eta'^2} \qquad \text{or} \qquad -\frac{\eta'\sqrt{(1 - a^2\eta^2)}}{2\eta} \left(\frac{1}{\eta - \eta'} - \frac{1}{\eta + \eta'} \right)$$

and so the dependence of $dw/d\eta$ on a can be taken outside the integration sign :

$$\frac{d}{d\eta} \left(\frac{w(\eta)}{KV} \right) = \frac{\sqrt{(1 - a^2\eta^2)}}{2\pi\eta} \int_{-1}^1 \frac{d}{d\eta'} \left(\frac{l(\eta')}{4K^2} \right) \left(\frac{1}{\eta - \eta'} - \frac{1}{\eta + \eta'} \right) d\eta' \quad .. \quad .. \quad (4)$$

$$= \sqrt{(1 - a^2\eta^2)} \left\{ \frac{d}{d\eta} \left(\frac{w(\eta)}{KV} \right) \right\}_{a=0} . \quad .. \quad .. \quad .. \quad .. \quad .. \quad (5)$$

Thus the derivative of the upwash at a Mach number greater than one is simply expressed in terms of the upwash producing the same load distribution at sonic speed. The upwash itself follows from the condition that all perturbation velocities vanish at the Mach cone, $\eta = 1/a$:

$$\frac{w(\eta)}{KV} = \int_{1/a}^{\eta} \sqrt{(1 - a^2\eta'^2)} \left\{ \frac{d}{d\eta'} \left(\frac{w(\eta')}{KV} \right) \right\}_{a=0} d\eta' . \quad .. \quad .. \quad .. \quad .. \quad (6)$$

4

Since $dl/d\eta'$ is odd, we may rewrite (4) as

$$\frac{\eta}{\sqrt{(1-a^2\eta^2)}}\frac{d}{d\eta}\left(\frac{w(\eta)}{KV}\right) = \frac{1}{\pi}\int_{-1}^{1}\frac{d}{d\eta'}\left(\frac{l(\eta')}{4K^2}\right)\frac{d\eta'}{\eta-\eta'}. \qquad \cdots \qquad \cdots \qquad \cdots \qquad (7)$$

Note that for $dw/d\eta$ to be finite at $\eta=0$ we require

$$\int_{-1}^{1}\frac{d}{d\eta'}\left(\frac{l(\eta')}{4K^2}\right)\frac{d\eta'}{\eta'} = 0. \qquad \cdots \qquad \cdots \qquad \cdots \qquad \cdots \qquad \cdots \qquad (8)$$

This condition is satisfied by all load distributions for which the spanwise distribution of chord loading is smooth at the centre-line.

2.2. *Inversion of the Integral Equation.*—Equation (7), regarded as an integral equation for $dl/d\eta'$, is related to Hilbert's integral equation, and has been dealt with in this form by Söhngen[13]. The solution is indeterminate to the extent of terms in $dl/d\eta'$ having singularities like $(1-\eta'^2)^{(1-2n)/2}$, which contribute nothing to the integral if $n>1$. Since we consider only functions l which vanish at the leading edge and since l is even, we can write the inverse of (7) as (*see* Ref. 13)

$$\frac{d}{d\eta'}\left(\frac{l(\eta')}{4K^2}\right) = \frac{1}{\pi\sqrt{(1-\eta'^2)}}\int_{-1}^{1}\frac{\eta\sqrt{(1-\eta^2)}}{\sqrt{(1-a^2\eta^2)}}\frac{d}{d\eta}\left(\frac{w}{KV}\right)\frac{d\eta}{\eta-\eta'}. \qquad \cdots \qquad \cdots \qquad (9)$$

By integration of (9) with respect to η', we find

$$\frac{l(\eta')}{4K^2} = \frac{1}{\pi}\int_{-1}^{1}\frac{\eta}{\sqrt{(1-a^2\eta^2)}}\frac{d}{d\eta}\left(\frac{w}{KV}\right)\log\left|\frac{1-\eta\eta'+\sqrt{\{(1-\eta^2)(1-\eta'^2)\}}}{\eta-\eta'}\right|d\eta \qquad (10)$$

where the integration constant has been determined by the condition $l(1)=0$. Equation (10) apparently specifies l in terms of $dw/d\eta$ only, which is absurd. In fact (10) prescribes just one of the load distributions corresponding to the single infinity of upwash distributions having the same derivative, namely that one which vanishes at the leading edge. Thus (10) gives the load distribution on the cambered wing when it is at the incidence at which the attachment line of the flow is at the leading edge. If the incidence is increased by α the load distribution is increased by $4K\alpha/\{E(k)\sqrt{(1-\eta^2)}\}$, where E is the complete elliptic integral of the second kind of modulus $k=\sqrt{(1-a^2)}$.

2.3. *Minimum Lift-Dependent Drag for Delta Wings at Sonic Speed or Slender Delta Wings.*— Before continuing the discussion of the conically-cambered wing on the basis of supersonic linearized theory, we consider the special case $a=0$, which may be regarded as applying to vanishingly slender wings at any Mach number or to wings of finite aspect ratio at $M=1$. This simplification permits a more complete discussion than can be given for non-zero values of a and forms a useful introduction to the subsequent treatment in Section 2.4.

We consider a conically-cambered slender delta wing having a load distribution {*cf.* (I.12) of Appendix I}.

$$4K^2\sum_1^{\infty}c_n\left(2n\sin(2n-1)\psi + (2n-1)\frac{\cos 2n\psi}{\sin\psi}\right) = \frac{4K^2\sum_1^{\infty}(2n-1)c_n}{\sin\psi} + l(\eta) \qquad \cdots \qquad (11)$$

where $\psi=\cos^{-1}\eta$, c_n is constant independent of x, and

$$l(\eta) = 4K^2\sum_1^{\infty}c_n\left(2n\sin(2n-1)\psi - (2n-1)\frac{1-\cos 2n\psi}{\sin\psi}\right) \qquad \cdots \qquad \cdots \qquad (12)$$

is a symmetrical load distribution vanishing at the leading edge. The first term on the right-hand side of (11) is a flat-plate loading corresponding to the upwash

$$-KV\sum_1^{\infty}(2n-1)c_n. \qquad \cdots \qquad \cdots \qquad \cdots \qquad \cdots \qquad \cdots \qquad \cdots \qquad (13)$$

5

The second term $l(\eta)$ corresponds to an upwash which we find by the method of Section 2.1. Let a tend to zero in (3), assuming (8) holds, giving

$$\frac{w(\eta)}{KV} = \frac{1}{\pi} \int_{-1}^{1} \frac{d}{d\eta'} \left(\frac{l(\eta')}{4K^2} \right) \log \frac{\sqrt{|\eta^2 - \eta'^2|}}{|\eta|} \frac{d\eta'}{\eta'}$$

$$= \frac{1}{\pi} \int_{-1}^{1} \frac{l^*(\eta')}{4K^2} \frac{d\eta'}{\eta - \eta'} \quad \cdots \quad \cdots \quad \cdots \quad \cdots \quad \cdots \quad \cdots \quad (14)$$

where

$$l^*(\eta') = \int_{0}^{\eta'} \frac{dl}{d\eta} \frac{d\eta}{\eta} = \int_{\pi/2}^{\psi'} \frac{dl}{d\psi} \frac{d\psi}{\cos\psi} \quad \cdots \quad \cdots \quad \cdots \quad \cdots \quad \cdots \quad \cdots \quad (15)$$

and we have carried out an integration by parts and used the anti-symmetry of l^*. When l is given by (12), equation (8) does hold and we have

$$\frac{l^*(\eta')}{4K^2} = \sum_{1}^{\infty} (2n - 1) c_n \frac{\cos (2n - 1)\psi' - \cos \psi'}{\sin \psi'} \quad \cdots \quad \cdots \quad \cdots \quad \cdots \quad (16)$$

as may be verified by differentiation. Thus from (14) and (16), using Glauert's formula, we obtain an upwash

$$w(\eta) = \frac{KV}{\pi} \int_{0}^{\pi} \sum_{1}^{\infty} (2n - 1) c_n \frac{\cos (2n - 1)\psi' - \cos \psi'}{\cos \psi - \cos \psi'} d\psi'$$

$$= KV \sum_{1}^{\infty} (2n - 1) c_n \left(1 - \frac{\sin (2n - 1)\psi}{\sin \psi} \right). \quad \cdots \quad \cdots \quad \cdots \quad \cdots \quad (17)$$

Combining (13) and (17) to find the upwash produced by (11), we have

$$- KV \sum_{1}^{\infty} (2n - 1) c_n \frac{\sin (2n - 1)\psi}{\sin \psi}. \quad \cdots \quad \cdots \quad \cdots \quad \cdots \quad \cdots \quad (18)$$

Provided the series converge, (11) and (18) are the load and upwash on a conically-cambered delta wing. The lift coefficient is given by

$$C_L = \frac{1}{2} \int_{-1}^{1} 4K^2 \sum_{1}^{\infty} c_n \left(2n \sin (2n - 1)\psi + (2n - 1) \frac{\cos 2n\psi}{\sin \psi} \right) d\eta = 2\pi c_1 K^2. \quad (19)$$

The coefficient of drag due to the pressure integral, neglecting any singularity at the leading edge, is

$$C_{DP} = \frac{1}{2} \int_{-1}^{1} 4K^3 \sum_{n=1}^{\infty} c_n \left(2n \sin (2n - 1)\psi + (2n - 1) \frac{\cos 2n\psi}{\sin \psi} \right) \sum_{m=1}^{\infty} (2m - 1) c_m \sin \frac{(2m - 1)\psi}{\sin \psi} d\eta$$

$$= 2\pi \left\{ \sum_{n=1}^{\infty} n (2n - 1) c_n^2 + \sum_{n=1}^{\infty} \sum_{m=1}^{\infty} (2n - 1)(2m - 1) c_n c_m \right\} K^3. \quad \cdots \quad \cdots \quad (20)$$

This is alleviated by the coefficient of suction force due to the singularity at the leading edge. This is due to the first term on the right-hand side of (11) and, by flat-plate theory, has the value :

$$C_S = \pi K^3 \left(\sum_{n=1}^{\infty} (2n - 1) c_n \right)^2. \quad \cdots \quad \cdots \quad \cdots \quad \cdots \quad \cdots \quad \cdots \quad (21)$$

Thus the coefficient of lift-dependent drag is given by :

$$C_{Di} = C_{DP} - C_S = \pi K^3 \sum_{n=1}^{\infty} (2n - 1) c_n^2. \quad \cdots \quad \cdots \quad \cdots \quad \cdots \quad (22)$$

Now consider the quantity

$$\varkappa = \frac{\pi A C_{D\,i}}{C_L{}^2} = \frac{4\pi K C_{D\,i}}{C_L{}^2} = 1 + \sum_{n=2}^{\infty} (2n-1)\left(\frac{c_n}{c_1}\right)^2 . \qquad \cdots \qquad \cdots \qquad \cdots \qquad \cdots \qquad (23)$$

The flat plate is given by $c_n = 0$, $n \geqslant 2$ {see equation (18)} and thus $\varkappa$ attains its minimum for the flat plate. In this case the suction force is equal to the lift-dependent drag {equations (21) and (22)}. We are concerned with achieving a low value of $\varkappa$ without relying on any suction force whatever and so deal with the case $C_S = 0$, i.e., the attachment line is at the leading edge. We consider the case $c_n = 0$ for $n > N$, so as to obtain a finite number of parameters. Then we require

$$\varkappa = 1 + \sum_{n=2}^{N} (2n-1)\left(\frac{c_n}{c_1}\right)^2$$

to be a minimum, subject to the condition that C_S vanishes, i.e.,

$$g = 2 \sum_{n=1}^{N} (2n-1)\frac{c_n}{c_1} = 0 .$$

This is given by the solution of the N equations

$$\frac{\partial}{\partial c_n} (\varkappa + \lambda g) = 2(2n-1)\frac{c_n}{c_1{}^2} + 2\lambda(2n-1)\frac{1}{c_1} = 0 \qquad 2 \leqslant n \leqslant N$$

$$g = 2 \sum_{n=2}^{N} (2n-1)\frac{c_n}{c_1} + 2 = 0 .$$

The solution is

$$\frac{c_n}{c_1} = -\lambda = -\frac{1}{N^2-1} \text{ for } 2 \leqslant n \leqslant N ,$$

and we took

$$\frac{c_n}{c_1} = 0 \qquad\qquad \text{for } N < n .$$

Substituting these values in (23) we obtain the least value of $\varkappa$ that can be obtained using N terms and satisfying $C_S = 0$, viz.,

$$\varkappa_N = 1 + \frac{1}{N^2-1} . \qquad \cdots \qquad \cdots \qquad \cdots \qquad \cdots \qquad \cdots \qquad \cdots \qquad \cdots \qquad \cdots \qquad (24)$$

The corresponding values of the upwash and load distribution are given by (18) and (11) as

$$\frac{w_N}{c_1 KV} = -1 + \sum_{n=2}^{N} \frac{2n-1}{N^2-1} \frac{\sin(2n-1)\psi}{\sin\psi}$$

$$= -1 - \frac{1}{N^2-1} + \frac{(2N+1)\sin(2N-1)\psi - (2N-1)\sin(2N+1)\psi}{4(N^2-1)\sin^3\psi} \qquad (25)$$

$$\frac{l_N}{4K^2 c_1} = \frac{1}{\sin\psi} - \sum_{n=2}^{N} \frac{1}{N^2-1}\left(2n\sin(2n-1)\psi + (2n-1)\frac{\cos 2n\,\psi}{\sin\psi}\right)$$

$$= \frac{1}{\sin\psi} - \frac{N\sin 2\psi \sin 2N\psi + \cos 2\psi \cos 2N\psi - 1}{2(N^2-1)\sin^3\psi} . \qquad \cdots \qquad \cdots \qquad \cdots \qquad (26)$$

These functions are plotted in Figs. 3 and 4 for $N = 2, 3, 4$ and 5. From (24) we see that $\varkappa_N$ tends to one, the flat-plate value, as N tends to infinity, so that values of $\varkappa$ as close to the minimum as we please may be obtained with attachment at the leading edge. The convergence of the series (25) and (26) is not uniform and the limits of w_N and l_N are discontinuous.

7

For $0 < \psi < \pi$ we have, as $N \to \infty$,

$$\frac{w_N}{c_1 K V} \to -1, \qquad \frac{l_N}{4K^2 c_1} \to \frac{1}{\sin \psi}$$

which are the flat-plate values. However, for $\psi = 0$ or π, we have

$$\frac{w_N}{c_1 K V} = \frac{N(4N+1)}{3(N+1)}, \qquad \frac{l_N}{4K^2 c_1} = 0.$$

We obtain the wing surface from the relation

$$z(x, y) - z_l(y) = \int_{x_l(y)}^{x} \frac{\partial z(x', y)}{\partial x'} \, dx' \qquad .. \qquad .. \qquad .. \qquad .. \qquad .. \qquad .. \qquad .. \qquad .. \qquad (27)$$

where the integration is for constant y, z is the ordinate of the wing surface at (x, y), z_l is the ordinate of the leading edge at $\{x_l(y), y\}$ (with $x_l = |y|/K$). Since $y = Kx \cos \psi$ and $\partial z/\partial x = w/V$ we find, for the starboard half-wing :

$$\frac{z - z_l(y)}{s} = \cos \psi \int_0^{\psi} \frac{w(\eta')}{KV} \frac{\sin \psi'}{\cos^2 \psi'} \, d\psi' . \qquad .. \qquad .. \qquad .. \qquad .. \qquad .. \qquad .. \qquad .. \qquad (28)$$

Using (25), we find after some manipulation :

$$\frac{z_N - z_{Nl}}{c_1 s} = -\frac{N(1 - |\eta|)}{N + (-1)^{N+1}} - \frac{|\eta|}{N^2 - 1} \sum_{m=1}^{N-1} \sum_{n=m+1}^{N} (-)^{m+n} (1 - |\eta|^{2m-1}) \frac{2n-1}{2m-1} \times$$

$$\times \frac{\{(2n-1)^2 - 1^2\}\{(2n-1)^2 - 3^2\} \ldots \{(2n-1)^2 - (2m-1)^2\}}{(2m)!} \qquad .. \qquad (29)$$

The function $z_{Nl}(y)$ is arbitrary and may be chosen so as to fit, say, the leading or trailing edge to a prescribed curve. However, a conical wing is the simplest choice and for this z/s is a function of η only. Hence we are led to write $z_l/s = m|\eta|$. The parameter m may be adjusted, say to remove the kink in the wing cross-section at the centre-line, but we prefer to put $m = -c_1$ and so fix the leading edge to coincide with that of a flat plate producing the same lift. The function $z_N/c_1 s$ is plotted in Fig. 5 for $N = 2, 3, 4$ and 5. In Appendix II this simpler expression for $z_N/c_1 s$ on the starboard half-wing is obtained :

$$\frac{z_N}{c_1 s} = -1 - \frac{1}{N^2 - 1} \sum_{n=2}^{N} (-)^n (2n - 1) -$$

$$- \frac{4 \cos \psi}{N^2 - 1} \sum_{n=1}^{N-1} (-)^{N-n} \left[\frac{N-n+1}{2} \right] \{2N + (-1)^{N-n}\} \frac{1 - \cos (2n-1)\psi}{2n-1} \qquad (30)$$

where the square brackets signify the integral part of the enclosed expression. From this we see in Appendix II that $z_N/c_1 s \to -1$ at $N \to \infty$, the flat plate producing the same lift, as we should expect.

The chord loading is obtained as

$$L(y) = \int_{x_l}^{x} l \, dx = s \cos \psi \int_0^{\psi} \frac{l(\eta) \sin \psi' \, d\psi'}{K \cos^2 \psi'}$$

and so

$$\frac{L_N(y)}{c_1 K s} = 4 \sin \psi \left(1 - \frac{\sin (N+1)\psi + \sin (N-1)\psi}{(N^2 - 1) \sin^2 \psi} \right) \qquad .. \qquad .. \qquad .. \qquad .. \qquad (31)$$

as may be verified by differentiation. This function is plotted in Fig. 6. The explicit expressions for the upwash, surface shape, load distribution and chord loading in terms of $\eta = \cos \psi$ are given in Appendix III for $N = 2, 3, 4$ and 5.

8

An independent treatment of the conically-cambered slender delta wing by complex function theory is given in Appendix I.

2.4. *Minimum Lift-Dependent Drag for Delta Wings at Supersonic Speeds with Attachment at the Subsonic Leading Edges.*—Having completed our investigation of the conically-cambered slender delta wing ($a = 0$) in the previous section, we now turn to the case of supersonic flow with subsonic or sonic leading edges ($0 < a \leqslant 1$). We use the relations of Section 2.1 connecting conical load and upwash distributions when the leading edge is an attachment line to find camber surfaces of low lift-dependent drag subject to this condition.

We have at once that, in the absence of a leading-edge singularity,

$$C_{Di} = C_{DP} = -\int_0^1 l(\eta)\,\frac{\partial z}{\partial x}\,d\eta = -\int_0^1 l(\eta)\,\frac{w(\eta)}{V}\,d\eta . \qquad .. \qquad .. \qquad .. \qquad .. \quad (32)$$

Referring to equation (3), we see that, for the load distributions behaving like $(1 - \eta^2)^{1/2}$ at the leading edge found in Section 2.3, the upwash is given by an elliptic integral. Thus the complete analysis possible in the case $a = 0$ is unlikely to be achieved and has not been attempted. We consider a finite set of load distributions $l^{(n)}$ ($2 \leqslant n \leqslant N$), vanishing at the leading edge, and the corresponding downwash distributions $w^{(n)}$, given by (3).

Then, if

$$l = \sum_2^N \lambda_n\, l^{(n)} ,$$

we have

$$w = \sum_2^N \lambda_n\, w^{(n)}$$

and

$$C_{Di} = -\sum_{n=2}^N \sum_{m=2}^N \lambda_n\, \lambda_m \int_0^1 l^{(n)}(\eta)\,\frac{w^{(m)}(\eta)}{V}\,d\eta , \qquad .. \qquad .. \qquad .. \quad (33)$$

while

$$C_L = \sum_{n=2}^N \lambda_n \int_0^1 l^{(n)}(\eta)\,d\eta .$$

Thus we can consider $\varkappa = \pi A C_{Di}/C_L^2$ as a function of $\lambda_2, \ldots \lambda_N$ and minimize it with respect to them for constant C_L.

The first approach was to use a modification of (3) *viz.*,

$$\frac{w}{KV} - \sqrt{(1 - a^2\eta^2)}\,\frac{w}{KV}\bigg|_{a=0} = -\frac{1}{\pi}\int_{-1}^1 \frac{d}{d\eta'}\left(\frac{l(\eta')}{4K^2}\right)\Bigg\{\sqrt{(1 - a^2\eta'^2)}\log\frac{\sqrt{(1 - a^2\eta^2)} + \sqrt{(1 - a^2\eta'^2)}}{a\sqrt{|\eta^2 - \eta'^2|}} +$$

$$+ \sqrt{(1 - a^2\eta^2)}\log\sqrt{\left(\frac{|\eta^2 - \eta'^2|}{1 - \eta^2}\right)} - \sqrt{(1 - a^2)}\log\frac{\sqrt{(1 - a^2\eta^2)} + \sqrt{(1 - a^2)}}{a\sqrt{(1 - \eta^2)}}\Bigg\}\frac{d\eta'}{\eta'} \qquad .. \quad (34)$$

derived by the use of (8). This enables $w(\eta)/KV$ to be calculated by numerical integration for $0 \leqslant \eta < 1$, for a given function $l(\eta)$ for which the upwash at $a = 0$ is known. A further numerical integration produces the coefficient of $\lambda_m \lambda_n$ in (33). Unfortunately, it is necessary to know these coefficients accurately for the minimization of $\varkappa$ and this makes the labour of the numerical integrations required prohibitive.

It was therefore decided to work from equation (6). This gives the upwash corresponding to a load distribution l in terms of the upwash corresponding to the same load distribution at $a = 0$. Since, for the load distributions behaving like $(1 - \eta^2)^{1/2}$ at the leading edge, the

9

upwash at $a = 0$ only involves a square-root singularity off the wing ($1 \leqslant \eta \leqslant 1/a$) ; equation (6) shows that the upwash becomes the sum of a complete elliptic integral and an algebraic function of η. This algebraic function is simply the product of a polynomial and $\sqrt{(1 - a^2\eta^2)}$, so that the coefficient of $\lambda_n\lambda_m$ in (33) can be obtained explicitly in terms of the complete elliptic integrals of the first and second kinds. For actual calculation recurrence formulae were used in preference to the complicated polynomials. The details of the method and the expressions found are given in Appendix IV. Unfortunately the numerical procedure breaks down for small values of a, owing to the occurrence of high powers of a as denominators in the expressions.

For small values of a we expand equation (6) after integrating it by parts. This enables us to carry out an analysis like that of Section 2.3 with a term in a^2 included. Details of the method are given in Appendix VI. This approach covers the gap left between $a = 0$ and the lower limit of the numerical procedure described above, so that a minimum value of the lift-dependent drag, using a finite number of terms, can be found throughout the range $0 \leqslant a \leqslant 1$.

Calculations of the lift-dependent drag factor $\varkappa$ were carried out for $a = \sin 15, 30, 45, 60, 75, 90$ deg for optimum load and upwash distributions for $N = 2, 3$ and 4. The results are shown in Fig. 7, with the flat-plate values (assuming attached flow) for comparison.

The optimum load distributions for $N = 3$ for $a = \sin 30, 60, 90$ deg are compared in Fig. 8, the curve for $a = 0$ being indistinguishable from that for $a = \sin 30$ deg on this scale. For $N = 2$ there is no variation with a of the optimum load distribution and it is given in Fig. 4. The corresponding upwash distributions are shown in Fig. 9.

2.5. *The Delta Wing with Hinged Flaps at the Subsonic Leading Edges.*—The solution for the flat plate at incidence with leading-edge flaps hinged along lines through the apex, deflected symmetrically or anti-symmetrically, has been given by Shaw[14]. We shall use his results for symmetrical deflection downwards in the subsonic leading-edge case as an example of conical camber. The condition that the leading edge should be an attachment line imposes a single condition connecting incidence, flap deflection and hinge position. Thus, for each value of $a = \beta K$ and the lift coefficient, we obtain a family of wings as the hinge line varies. The singularity in the load distribution which occurs along the hinge line introduces the possibility of a flow separation along it on the upper surface. This singularity is, however, logarithmic, in contrast to the square-root singularity at the leading edge of the flat plate which is associated with the primary separation. Thus we shall suppose, in the absence of experimental evidence, that the flow remains attached at the hinge line. A small modification of the shape near the hinge line would in any case produce a non-singular load distribution and little change in the characteristics of the wing.

For a flat plate at zero incidence, with subsonic leading edge, having flaps hinged along the lines $\eta = \pm \bar{\eta}$ and deflected to an incidence ξ to the free stream, the pressure distribution is (*see* Section 5.22 of Ref. 14) :

$$p = - \rho V^2 \frac{\xi \bar{\eta} \tan \gamma}{\pi \sqrt{(1 - a^2\bar{\eta}^2)}} \left\{ \frac{2a^2 \sqrt{(1 - \bar{\eta}^2)} \Pi}{\sqrt{(1 - \eta^2)} E} + \log \left| \frac{\sqrt{(1 - \bar{\eta}^2)} - \sqrt{(1 - \eta^2)}}{\sqrt{(1 - \bar{\eta}^2)} + \sqrt{(1 - \eta^2)}} \right| \right\} \quad (35)$$

where $E = E(k)$, $k^2 = 1 - a^2$, is the complete elliptic integral of the second kind and

$$\Pi = \Pi(a^2\bar{\eta}^2 - 1, k) = \int_0^{\pi/2} \frac{d\psi}{\{1 - (1 - a^2\bar{\eta}^2) \sin^2 \psi\}\{1 - k^2 \sin^2 \psi\}^{1/2}}$$

is a complete elliptic integral of the third kind. For the flat plate at incidence α the pressure distribution is :

$$p = - \rho V^2 \frac{\alpha \tan \gamma}{\sqrt{(1 - \eta^2)} E} . \qquad .. \qquad .. \qquad .. \qquad .. \qquad .. \quad (36)$$

10

For no singularity at the leading edge, $\eta = 1$, we must combine (35) and (36), i.e., incidence and deflection, so that

$$\alpha = -\frac{\xi}{\pi} 2a^2 \Pi \frac{\bar{\eta}\sqrt{(1-\bar{\eta}^2)}}{\sqrt{(1-a^2\bar{\eta}^2)}} \cdot \qquad .. \qquad .. \qquad .. \qquad .. \qquad (37)$$

The non-dimensional load distribution is then

$$l = -\frac{2p}{\frac{1}{2}\rho V^2} = \frac{4\xi\bar{\eta}\tan\gamma}{\pi\sqrt{(1-a^2\bar{\eta}^2)}} \log \left| \frac{\sqrt{(1-\bar{\eta}^2)} - \sqrt{(1-\eta^2)}}{\sqrt{(1-\bar{\eta}^2)} + \sqrt{(1-\eta^2)}} \right| . \qquad .. \qquad (38)$$

Now

$$\int \log \left| \frac{\sqrt{(1-\bar{\eta}^2)} - \sqrt{(1-\eta^2)}}{\sqrt{(1-\bar{\eta}^2)} + \sqrt{(1-\eta^2)}} \right| d\eta = \eta \log \left| \frac{\sqrt{(1-\bar{\eta}^2)} - \sqrt{(1-\eta^2)}}{\sqrt{(1-\bar{\eta})^2} + \sqrt{(1-\eta^2)}} \right| - 2\sqrt{(1-\bar{\eta}^2)} \sin^{-1}\eta +$$

$$+ \bar{\eta} \log \left| \frac{\bar{\eta}\sqrt{(1-\eta^2)} + \eta\sqrt{(1-\bar{\eta}^2)}}{\bar{\eta}\sqrt{(1-\eta^2)} - \eta\sqrt{(1-\bar{\eta}^2)}} \right| \qquad .. \qquad .. \qquad (39)$$

as may be verified by differentiation. We have, in general,

$$C_L = \int_0^1 l(\eta) \, d\eta$$

and

$$C_{DP} = -\int_0^1 l(\eta) \frac{\partial z}{\partial x} \, d\eta \ .$$

Here, $C_{DP} = C_{Di}$, by (37), and

$$-\frac{\partial z}{\partial x} = \begin{cases} \alpha & \text{for } |\eta| < \bar{\eta} \\ \alpha + \xi & \text{for } \bar{\eta} < |\eta| < 1 \ . \end{cases} \qquad .. \qquad .. \qquad .. \qquad .. \qquad (40)$$

Thus, by (38), (39) and (40)

$$C_L = -\frac{4\xi\bar{\eta}\tan\gamma\sqrt{(1-\bar{\eta}^2)}}{\sqrt{(1-a^2\bar{\eta}^2)}} \qquad .. \qquad .. \qquad .. \qquad .. \qquad (41)$$

and

$$C_{Di} = \frac{8\xi^2\bar{\eta}\tan\gamma}{\pi\sqrt{(1-a^2\bar{\eta}^2)}} \left\{ \frac{a^2\Pi\bar{\eta}(1-\bar{\eta}^2)}{\sqrt{(1-a^2\bar{\eta}^2)}} - \sqrt{(1-\bar{\eta}^2)}\cos^{-1}\bar{\eta} - \bar{\eta}\log\bar{\eta} \right\} \qquad (42)$$

where (37) has been used for α. Thus we find

$$\varkappa = \frac{\pi A C_{Di}}{C_L^2} = 2a^2\Pi - 2\sqrt{\frac{(1-a^2\bar{\eta}^2)}{1-\bar{\eta}^2}} \left\{ \frac{\cos^{-1}\bar{\eta}}{\bar{\eta}} + \frac{\log\bar{\eta}}{\sqrt{(1-\bar{\eta}^2)}} \right\} . \qquad .. \qquad (43)$$

This has been calculated for $\sin^{-1}a = 0, 15, 30, 45, 60, 75, 85, 90$ deg for a range of hinge-line positions, $\bar{\eta}$. The results are shown in Figs. 10 and 11. The upwash on the wing with a flap is a step function; the load distribution has a logarithmic singularity at the hinge-line. In Figs. 12 and 13 the upwash and load distribution on the wing with flap at $a = 0$, $\bar{\eta} = 0 \cdot 966$ are compared with those derived for slender wings using five terms of the Fourier series (w_5 and l_5 of Appendix III) in Section 2.3. These cases were chosen since they produce similar values of $\varkappa$.

3. *Results.*—3.1. *The Lift-Dependent Drag Factor $\varkappa$.*—The lift-dependent drag factor :

$$\varkappa = \frac{\pi A C_{Di}}{C_L^2}$$

is plotted in Fig. 7 against the parameter $a = \tan\gamma/\tan\mu$ (apex angle 2γ, Mach angle μ) for $0 \leqslant a \leqslant 1$ for three types of cambered wing and the flat plate. Each cambered wing has leading-edge attachment, i.e., no infinity of the loading at the leading edge and so no localized leading-edge suction. The curves labelled $N = 2, 3, 4$ in Fig. 7 give the minimum values of $\varkappa$ obtainable using that number of terms of a trigonometrical series for the load distribution and maintaining leading-edge attachment.

11

It is seen that conically-cambered wings with leading-edge attachment exist for $0 \leqslant a \leqslant 1$ having values of $\varkappa$ close to that of the flat plate at design incidence and Mach number. We know from Section 2.3 equation (24) that, for $a = 0$, a family of wings can be found for which $\varkappa$ is as near the flat-plate value (*i.e.*, 1) as we please. The analysis of Appendix VI, in particular equation (VI.12) suggests that the same is true for small values of a. For values of a which are just below one, the theory predicts an appreciable reduction of $\varkappa$ below the flat-plate value ; but linearized theory is not likely to be reliable in this range since the bow shock is close to the leading edge. For $a = 0$, the flat-plate value cannot be improved upon in attached flow past a substantially plane* wing, so that for slender wings the penalty in the lift-dependent drag due to achieving leading-edge attachment by conical camber can be made as small as we please at design incidence. (This is under the assumption that the theory is applicable, a point discussed in Section 3.2.) For other values of a the restriction to conical camber as a means of securing leading-edge attachment probably does involve a penalty in the lift-dependent drag, but at least the flat-plate value can be approached.

In the special case of conical camber represented by a delta wing with a hinged leading-edge flap, the condition of leading-edge attachment determines the flap deflection once the hinge-line is fixed. In Fig. 10 the values of $\varkappa$ for various hinge-line positions ($\bar{\eta}$) are shown for $0 \leqslant a \leqslant 1$. As the hinge-line approaches the leading edge the flat-plate value is approached and the latter is only improved upon with hinge-lines near the leading edge when this is nearly sonic and the theory is then inadequate. The curves are not taken beyond the values for $\varkappa$ obtained by omitting the suction force in the flat-plate solution. Fig. 11 is a cross-plot of the curves in Fig. 10 and shows for several values of a the dependence of $\varkappa$ on hinge-line position.

3.2. *The Optimised Load and Upwash Distributions.*—Figs. 3 and 4, for the case $a = 0$, illustrate the trend of the optimised upwash and load distributions as more terms are included in the trigonometrical series for the load distribution, at least for values of a not too near 1. Apart from the introduction of more ' waviness '† into the functions, the tendency is for the downwash to approach the constant flat-plate value, except at the leading edge where there is an increasing upwash, and for the load to approach the flat-plate distribution, except at the leading edge where it is zero. The large upwash near the leading edge means a high surface slope, so that linear theory ceases to be applicable when N becomes too large. (The significance of ' too ' depends on the design lift coefficient and the sweep, so no attempt at precision is made.) The high suction peak and the adverse pressure gradient inboard of it may lead to the occurrence of shock waves and to boundary-layer separation, so that again linear theory will not apply when N is too large.

The cross-sections of particular conical wings having the upwash distributions shown in Fig. 3 are given in Fig. 5. They have been chosen to have the same leading edge for all N, and can be seen to approach the flat plate as $N \rightarrow \infty$. The increasing surface slope near the leading edge as N increases is evident. The chord loading of the same wings is compared with the elliptic loading in Fig. 6. The differences from the elliptic loading are associated with the increases in vortex drag above the minimum.

The effect of increasing Mach number on the optimised load and upwash distributions can be seen in Figs. 8 and 9. There is little change in the load distributions, particularly for small values of a, so that the optimum distribution at $a = 0.50$ for $N = 3$ is indistinguishable from that at $a = 0$ on the scale used. The tendency is for the load to be spread rather more evenly across the span as a increase from 0 to 1. Similarly, the difference in the upwash distribution

---

* A substantially plane wing here means a wing close enough to a plane for the boundary condition satisfied on the wing to be applied on the plane. Thus wings with end-plates, ring wings, etc., are excluded.

† This waviness, due to the representation of the load distribution by Fourier terms, is incidental, as is brought out by some work of Brebner[15]. He calculates the load distributions and lift-dependent drag factors of slender wings having leading-edge attachment and downwash distributions without points of inflexion. His results are of a similar nature to those given here.

between $a = 0$ and $0 \cdot 50$ is almost a constant, corresponding to a change in incidence only (Fig. 9). However, for larger values of a the change in upwash is greater near the leading edge than at the centre-line. When the leading edge is sonic the upwash vanishes at the leading edge, as we should expect since we have required the load to vanish there and the solution should be continuous with that for a supersonic leading edge.

Figs. 12 and 13 show the continuity of the results for the hinged flap with those for the smoothly cambered wing at $a = 0$. The cases $N = 5$ and $\bar{\eta} = 0 \cdot 966$ were chosen for comparison since they yield substantially the same value of $\varkappa$. It can be seen that the step function of Fig. 13 approximates fairly closely to the smooth curve ; and that the singular load distribution in Fig. 12 is similar to the continuous one if we bear in mind that the singularity is logarithmic and so has little effect on the overall distribution.

An impression of the streamlines in the cross-flow (*i.e.*, the lines $\Psi = \mathrm{const.}$, at equal intervals of Ψ where Ψ is the imaginary part of the complex potential W of Appendix I) for the case $a = 0$, $N = 2$ is given in Fig. 14b. The corresponding picture for the attached flow past the flat wing is Fig. 14a. The streamlines are drawn relative to the undisturbed stream, so that the velocity field dies out at large distances and a normal velocity is found at the (instantaneous) position of the wing. Only the intersections of the lines with the horizontal axis have been calculated, the remainder of the pictures being illustrative. There is a marked resemblance between the flow field for the cambered wing and for a flat wing of smaller span, the difference being that the streamlines are less closely crowded for the cambered wing. This comparison provides another way of envisaging the higher lift-dependent drag factor of the cambered wing on attached-flow theory, together with the greater likelihood of achieving attached flow on it in a real fluid.

4. *Conclusions.*—At sonic speed, the lift-dependent drag on a conically-cambered wing, with flow attachment at the leading edge (*i.e.*, vanishing load at the leading edge) at design incidence, can be reduced as near as we please to that of a flat plate producing the same lift, if the flow past the latter were not to separate.

The same appears to be true at supersonic speeds for wings having subsonic leading edges (calculations so far produce values within 5 per cent of the flat-plate value) unless the leading edge is almost sonic. For leading edges only just within the Mach cone from the apex, reductions of up to 7 per cent below the flat-plate value are found, but linear theory is unlikely to be reliable in this region.

These values are obtained for wings having upwash distributions which are finite everywhere on the wing and load distributions which vanish at the leading edge. The lower values of the lift-dependent drag factor are obtained with high values of the upwash on the wing near the leading edge and a high suction peak just inboard of it on the upper surface. However, these are proportional to the design lift coefficient, so that for a low lift coefficient it is probably permissible to apply linear theory to the wings calculated by this method which have lift-dependent drag factors very near the flat-plate value, since their steep surfaces slopes and the risk of shock waves and boundary-layer separation are reduced.

The load distributions obtained by minimizing the lift-dependent drag factor vary little with $a = \tan \gamma / \tan \mu$. The associated upwash increases with a ; the increment is nearly constant across the span except when the leading edge is almost sonic. This is paralleled by the decrease in lift-curve slope of a flat delta wing as a increases.

13

LIST OF SYMBOLS

a	$=$	$\beta K = \tan\gamma/\tan\mu$
A		Aspect ratio
c_n		Fourier coefficient {equation (11)}
C_L		Lift coefficient
C_{Di}		Induced drag coefficient
C_{DP}		Induced pressure-drag coefficient (suction neglected)
C_S		Suction-force coefficient
$E(k)$		Complete elliptic integral of the second kind, modulus k
k	$=$	$\sqrt{(1-a^2)}$
K	$=$	$A/4 = \tan\gamma$
$K(k)$		Complete elliptic integral of the first kind, modulus k
l		Non-dimensional load distribution
$L(y)$		Chord loading
M		Mach number
N		Number of Fourier terms considered
p		Pressure
s	$=$	Kx, local semi-span
v		Sidewash velocity
V		Undisturbed velocity
w		Upwash velocity
W		Complex potential
x, y, z		Right-handed rectangular co-ordinates, x parallel to the undisturbed velocity, y to starboard, z vertically upwards
Z	$=$	$y + iz$
α		Incidence
β	$=$	$\sqrt{(M^2-1)}$
2γ		Apex angle
η	$=$	y/s
$\bar{\eta}$		Hinge-line position
ζ	$=$	$Z + \sqrt{(Z^2-s^2)}$
$\varkappa$	$=$	$\pi A C_{Di}/C_L^2$ lift-dependent drag factor
λ		Lagrangian multiplier
μ	$=$	$\cot^{-1}\beta$, Mach angle
ξ		Relative incidence of deflected flap
Π		Complete elliptic integral of third kind
ρ		Density

14

LIST OF SYMBOLS—*continued*

Φ Velocity potential

$\phi \;=\; \cosh^{-1} \eta \;\; (\eta \geqslant 1)$

$\psi \;=\; \cos^{-1} \eta \;\; (\eta \leqslant 1)$

$\Psi \;=\; Im\{W\}$

REFERENCES

No.	Author	Title, etc.
1	K. W. Mangler and J. H. B. Smith	Calculation of the flow past a delta wing with leading edge separation. *Proc. Roy. Soc.* A. Vol. 251. p. 200. May, 1959.
2	E. C. Maskell	Flow separation in three dimensions. A.R.C. 18,063. November, 1955.
3	G. M. Roper	Use of camber and twist to produce low-drag delta or swept-back wings, without leading-edge singularities at supersonic speeds. A.R.C. R. & M. 3196. December, 1958.
4	G. M. Roper	Drag reduction of thin wings at supersonic speeds, by the use of camber and twist. A.R.C. R. & M. 3132. July, 1957.
5	R. T. Jones	The minimum drag of thin wings in frictionless flow. *J. Ae. Sci.* Vol. 18. No. 2. p. 75. February, 1951.
6	R. T. Jones	Theoretical determination of the minimum drag of airfoils at supersonic speeds. *J. Ae. Sci.* Vol. 19. No. 12. p. 813. December, 1952.
7	Mac. C. Adams and W. R. Sears	Slender body theory—review and extension. *J. Ae. Sci.* Vol. 20. No. 2. p. 85. February, 1953.
8	W. A. Tucker	A method for the design of sweptback wings warped to produce specified flight characteristics at supersonic speeds. N.A.C.A. Report 1226. 1955.
9	F. C. Grant	The proper combination of lift loadings for least drag on a supersonic wing. N.A.C.A. Report 1275. 1956.
10	J. W. Boyd, E. Migotsky and B. E. Wetzel	A study of conical camber for triangular and sweptback wings. N.A.C.A. Research Memo. A55G19. TIL 4877. November, 1955.
11	S. H. Tsien	The supersonic conical wing of minimum drag. *J. Ae. Sci.* Vol. 22. No. 12. p. 805. December, 1955.
12	M. A. Heaslet and H. Lomax	Supersonic and transonic small perturbation theory. *General Theory of High Speed Aerodynamics.* Section D. Editor, W. R. Sears. Oxford University Press, London, 1955.
13	H. Söhngen	Die Losüngen der Integralgleichung $g(x) = \dfrac{1}{2\pi} \displaystyle\int_{-a}^{a} \dfrac{f(\xi)\,d\xi}{x - \xi}$. *Mathematische Zeitschrift.* Vol. 45. p. 245. 1939.
14	B. W. B. Shaw	Nose controls on delta wings at supersonic speeds. College of Aeronautics, Cranfield, Report No. 36. A.R.C. 13,372. May, 1950.
15	G. G. Brebner	Some simple conical camber shapes to produce low lift-dependent drag on a slender delta wing. A.R.C. C.P. 428 September, 1957.

15

APPENDIX I

The Conically-Cambered Slender Delta Wing

We introduce the complex quantity $Z = y + iz$ in the cross-flow plane, in which the wing is represented by a distribution of normal velocity along the slit $|y| \leqslant s, z = 0$. Then the perturbation potential is the real part of a complex analytic function W of Z, containing x as a parameter. This potential vanishes at infinity, its conjugate function vanishes on the imaginary axis, the normal velocity is continuous across the slit and the velocity field has at most a square-root singularity at $z = \pm s$. We introduce a transformed plane ζ, defined by

$$\zeta = Z + \sqrt{(Z^2 - s^2)}, \qquad Z = \tfrac{1}{2}(\zeta + s^2/\zeta) . \qquad .. \qquad .. \qquad .. \quad (I.1)$$

The Z plane cut along the wing slit becomes the region of the ζ plane outside $|\zeta| = s$. Since in this region the transformation is analytic and one valued, and since a singularity in W on $|\zeta| = s$ would correspond to one on the wing slit, W is a one-valued analytic function outside and on $|\zeta| = s$, and we can write

$$\frac{W}{KVs} = \sum_{n=1}^{\infty} a_n \left(\frac{s}{\zeta}\right)^n \text{ for } |\zeta| \geqslant s . \quad .. \qquad .. \qquad .. \qquad .. \qquad .. \qquad .. \quad (I.2)$$

In this expression a_n is dimensionless and, by the assumption of a conical velocity field, independent of x. For W to vanish on the imaginary axis (Z imaginary corresponds to ζ imaginary),

$$a_{2n} = b_n , \qquad a_{2n-1} = ic_n , \quad b_n \text{ and } c_n \text{ real} .$$

Now

$$\frac{v - iw}{KV} = \frac{d\zeta}{dz} \frac{d}{d\zeta}\left(\frac{W}{KV}\right) = -\frac{2}{\zeta/s - s/\zeta} \sum_{n=1}^{\infty} n a_n \left(\frac{s}{\zeta}\right)^n .$$

On the wing, where $\zeta = se^{i\psi}$:

$$\frac{v - iw}{KV} = \frac{i}{\sin\psi} \sum_{n=1}^{\infty} n a_n e^{-ni\psi} .$$

Thus for w to be the same at $\pm\psi$ we require $b_n = 0$. Hence

$$\frac{W}{KVs} = \sum_{n=1}^{\infty} ic_n \left(\frac{s}{\zeta}\right)^{2n-1} \qquad .. \qquad .. \qquad .. \qquad .. \qquad .. \qquad .. \qquad .. \quad (I.3)$$

$$\frac{v - iw}{KV} = -\frac{2i\zeta s}{\zeta^2 - s^2} \sum_{n=1}^{\infty} (2n - 1) c_n \left(\frac{s}{\zeta}\right)^{2n-1} \qquad .. \qquad .. \qquad .. \qquad .. \quad (I.4)$$

and, in particular, on the wing

$$\frac{\Phi}{KVs} = \sum_{1}^{\infty} c_n \sin(2n - 1)\psi \qquad .. \qquad .. \qquad .. \qquad .. \qquad .. \qquad .. \quad (I.5)$$

$$\frac{v}{KV} = -\frac{1}{\sin\psi} \sum_{n=1}^{\infty} (2n - 1) c_n \cos(2n - 1)\psi \quad .. \qquad .. \qquad .. \qquad .. \quad (I.6)$$

$$\frac{w}{KV} = -\frac{1}{\sin\psi} \sum_{n=1}^{\infty} (2n - 1) c_n \sin(2n - 1)\psi . \quad .. \qquad .. \qquad .. \qquad .. \quad (I.7)$$

The lift is most readily found from the momentum integral in a plane behind the wing. In fact

$$\frac{C_L}{K^2} = 2 \int_{-1}^{1} \frac{\Delta\Phi}{KVs} d\eta = 2\pi c_1 . \quad .. \qquad .. \qquad .. \qquad .. \qquad .. \qquad .. \quad (I.8)$$

16

The lift-dependent drag, which for slender wing theory (*i.e.*, $a = 0$) is entirely vortex drag, is obtained from the energy integral in a plane behind the wing. We have

$$\frac{C_{Di}}{K^3} = \int_{-1}^{1} \frac{\Delta\Phi}{KVs} \frac{w}{KV} \cdot d\eta = \pi \sum_{n=1}^{\infty} (2n-1) c_n{}^2 \ldots \qquad \ldots \qquad \ldots \qquad \ldots \quad (I.9)$$

Thus we have :

$$\varkappa = \frac{\pi A C_{Di}}{C_L{}^2} = \frac{4\pi K C_{Di}}{C_L{}^2} = 1 + \sum_{n=2}^{\infty} (2n-1) \left(\frac{c_n}{c_1}\right)^2 \ldots \qquad \ldots \qquad \ldots \quad (I.10)$$

The condition for attachment to occur at the leading edge is that the velocity is finite there, *i.e.*,

$$\sum_{n=1}^{\infty} (2n-1) c_n = 0 \ldots \qquad \ldots \qquad \ldots \qquad \ldots \qquad \ldots \qquad \ldots \qquad \ldots \qquad \ldots \quad (I.11)$$

To find the load distribution on the wing, we note that v^2 and w^2 are continuous across the wing, and so the non-dimensional load distribution is

$$l = \frac{4}{V} \frac{\partial\Phi}{\partial x} , \text{ on the wing.}$$

Hence

$$\frac{l}{4K^2} = \sum_{1}^{\infty} c_n \left\{ 2n \sin (2n-1)\psi + (2n-1) \frac{\cos 2n\psi}{\sin \psi} \right\} \ldots \qquad \ldots \qquad \ldots \quad (I.12)$$

B

APPENDIX II

The Optimum Slender-Wing Shape, Using N Terms of the Fourier Series

We evaluate the wing shape $z(x, y)$ from equations (28) and (25).   First we find

$$J_m = \int_0^\psi \frac{\sin 2m\psi'}{\cos \psi'} \, d\psi' \ .$$

Since

$$\sin 2m\psi + \sin(2m - 2)\psi = 2 \sin(2m - 1)\psi \cos \psi$$

$$J_m = 2 \frac{1 - \cos(2m - 1)\psi}{2m - 1} - J_{m-1}$$

and so

$$J_m = 2 \sum_{v=1}^{m} (-)^{m-v} \frac{1 - \cos (2v - 1)\psi}{2v - 1} \quad (J_0 = 0) \ .$$

Now we find

$$I_n = \int_0^\psi \frac{\sin (2n - 1)\psi' \, d\psi'}{\cos^2\psi'} \ .$$

Since

$$\sin (2n - 1)\psi + \sin (2n - 3)\psi = 2 \sin 2(n - 1)\psi \cos \psi$$

$$I_n = 2J_{n-1} - I_{n-1}$$

and so

$$I_n = (-)^{n-1} I_1 + 2 \sum_{m=1}^{n-1} (-)^{n-m-1} J_m$$

$$= (-)^{n-1} \left\{ \sec \psi - 1 + 4 \sum_{m=1}^{n-1} \sum_{v=1}^{m} (-)^v \frac{1 - \cos (2v - 1)\psi}{2v - 1} \right\} \ .$$

Now, by (28), for the starboard half-wing :

$$\frac{z_N - z_l(y)}{c_1 s} = \cos \psi \int_0^\psi \frac{w(\eta')}{c_1 KV} \frac{\sin \psi'}{\cos^2 \psi'} \, d\psi'$$

$$= \cos \psi \int_0^\psi \left(-\frac{\sin \psi'}{\cos^2 \psi'} + \sum_2^N \frac{2n - 1}{N^2 - 1} \frac{\sin (2n - 1)\psi'}{\cos^2 \psi'} \right) d\psi' \text{ by (25)}$$

$$= \cos \psi \left(1 - \sec \psi + \frac{1}{N^2 - 1} \sum_2^N (2n - 1) I_n \right) ,$$

which becomes

$$\frac{z_N - z_l(y)}{c_1 s} = - (1 - \cos \psi) \left(1 + \frac{1}{N^2 - 1} \sum_{n=2}^N (-)^n (2n - 1) \right) +$$

$$+ \frac{4 \cos \psi}{N^2 - 1} \sum_{n=1}^{N-1} (-)^{N-n+1} \left[\frac{N - n + 1}{2} \right] (2N + (- 1)^{N-n}) \frac{1 - \cos (2n - 1)\psi}{2n - 1}$$

where $[m]$ denotes the integral part of m.   For the flat plate at the same lift, $z = -c_1 s$, so that if we choose $z_l(y) = -c_1 |y|$ the leading edges of the flat plate and cambered wing coincide. With this choice

$$\frac{z_N}{c_1 s} + 1 = - \frac{1}{N^2 - 1} \sum_{n=2}^N (-)^n (2n - 1) -$$

$$- \frac{4 \cos \psi}{N^2 - 1} \sum_{n=1}^{N-1} (-)^{N-n} \left[\frac{N - n + 1}{2} \right] (2N + (- 1)^{N-n}) \frac{1 - \cos (2n - 1)\psi}{2n - 1} \ .$$

As N tends to infinity, the right-hand side tends to zero and so

$$z_N \to -c_1 s \qquad \text{as} \qquad N \to \infty \ .$$

APPENDIX III

The Upwash, Surface Shape, Load Distribution and Chord Loading for Optimum Slender Delta Wings

$$\frac{w_2}{c_1 KV} = 2(2\eta^2 - 1)$$

$$\frac{z_2}{c_1 s} = -4\eta^2 + 5|\eta| - 2$$

$$\frac{l_2}{4K^2 c_1} = \frac{4}{3}(1 - \eta^2)^{1/2}(2\eta^2 + 1)$$

$$\frac{L_2}{4Kc_1 s} = \frac{4}{3}(1 - \eta^2)^{3/2}$$

$$\frac{w_3}{c_1 KV} = 10\eta^4 - 6\eta^2 - \frac{3}{4}$$

$$\frac{z_3}{c_1 s} = -\frac{10}{3}\eta^4 + 6\eta^2 - \frac{35}{12}|\eta| - \frac{3}{4}$$

$$\frac{l_3}{4K^2 c_1} = (1 - \eta^2)^{1/2}(8\eta^4 + 1)$$

$$\frac{L_3}{4Kc_1 s} = (1 - \eta^2)^{3/2}(2\eta^2 + 1)$$

$$\frac{w_4}{c_1 KV} = \frac{448}{15}\eta^6 - 32\eta^4 + 8\eta^2 - \frac{4}{3}$$

$$\frac{z_4}{c_1 s} = -\frac{448}{75}\eta^6 + \frac{32}{3}\eta^4 - 8\eta^2 + \frac{273}{75}|\eta| - \frac{4}{3}$$

$$\frac{l_4}{4K^2 c_1} = \frac{16}{15}(1 - \eta^2)^{1/2}(24\eta^6 - 12\eta^4 + 2\eta^2 + 1)$$

$$\frac{L_4}{4Kc_1 s} = \frac{16}{15}(1 - \eta^2)^{3/2}(4\eta^4 + 1)$$

$$\frac{w_5}{c_1 KV} = 96\eta^8 - \frac{448}{3}\eta^6 + 70\eta^4 - 10\eta^2 - \frac{5}{6}$$

$$\frac{z_5}{c_1 s} = -\frac{96}{7}\eta^8 + \frac{448}{3}\eta^6 - \frac{70}{3}\eta^4 + 10\eta^2 - \frac{209}{70}|\eta| - \frac{5}{6}$$

$$\frac{l_5}{4K^2 c_1} = (1 - \eta^2)^{1/2}\left(\frac{256}{3}\eta^8 - \frac{256}{3}\eta^6 + 24\eta^4 + 1\right)$$

$$\frac{L_5}{4Kc_1 s} = (1 - \eta^2)^{3/2}\left(\frac{32}{3}\eta^6 - \frac{16}{3}\eta^4 + 2\eta^2 + 1\right)$$

19

APPENDIX IV

Numerical Calculation of the Lift-Dependent Drag of the Conically-Cambered Delta Wing for $0 < a \leqslant 1$

We consider this set of upwash distributions on the wing which lead to wings with leading-edge attachment at $a = 0$:

$$
\left.\frac{w^{(2)}}{c_1 KV}\right|_{a=0} = 2(2\eta^2 - 1) \qquad \text{given by } \frac{c_2}{c_1} = -\frac{1}{3}, \frac{c_n}{c_1} = 0, n \neq 2, 1
$$

$$
\left.\frac{w^{(3)}}{c_1 KV}\right|_{a=0} = 4\eta^2(4\eta^2 - 3) \qquad \text{given by } \frac{c_3}{c_1} = -\frac{1}{5}, \frac{c_n}{c_1} = 0, n \neq 3, 1 \qquad \text{(IV.1)}
$$

$$
\left.\frac{w^{(4)}}{c_1 KV}\right|_{a=0} = 2(32\eta^6 - 40\eta^4 + 12\eta^2 - 1) \text{ given by } \frac{c_4}{c_1} = -\frac{1}{7}, \frac{c_n}{c_1} = 0, n \neq 4, 1
$$

The corresponding upwash distributions in the plane of the wing, but off it, are : {*see* equation (I.4) with $\zeta/s = \eta + \sqrt{(\eta^2 - 1)}$}

$$
\left.\frac{w^{(2)}}{c_1 KV}\right|_{a=0} = 2\{\eta - \sqrt{(\eta^2 - 1)^2}\}
$$

$$
\left.\frac{w^{(3)}}{c_1 KV}\right|_{a=0} = 4\eta\{\eta - \sqrt{(\eta^2 - 1)^3}\} \qquad \qquad \text{.. .. .. (IV.2)}
$$

$$
\left.\frac{w^{(4)}}{c_1 KV}\right|_{a=0} = 2(4\eta^2 - 1)\{\eta - \sqrt{(\eta^2 - 1)^4}\}
$$

The corresponding load distributions are : {*see* equation (I.12)}

$$
\frac{l^{(2)}}{4K^2 c_1} = \frac{4}{3} \sqrt{(1 - \eta^2)} (2\eta^2 + 1)
$$

$$
\frac{l^{(3)}}{4K^2 c_1} = \frac{4}{5} \sqrt{(1 - \eta^2)} (16\eta^4 - 2\eta^2 + 1) \qquad \qquad \text{.. .. .. .. (IV.3)}
$$

$$
\frac{l^{(4)}}{4K^2 c_1} = \frac{8}{7} \sqrt{(1 - \eta^2)} (48\eta^6 - 32\eta^4 + 4\eta^2 + 1)
$$

Then the upwash distributions at non-zero a which correspond to these load distributions are given by equation (6). The expression for $w^{(n)}/c_1 KV$ on the wing must be used in the range of integration $\eta \leqslant \eta' \leqslant 1$ and that for $w^{(n)}/c_1 KV$ off the wing in the range $1 \leqslant \eta' \leqslant 1/a$. From the former range we obtain an algebraic function of η and from the latter a complete elliptic integral. Thus, on the wing, with $k^2 = 1 - a^2$,

$$
\frac{w^{(2)}}{c_1 KV} = \frac{4}{3a^2} \{(2 - a^2) E(k) - a^2 K(k) - 2(1 - a^2\eta^2)^{3/2}\}
$$

$$
\frac{w^{(3)}}{c_1 KV} = \frac{4}{15a^4} \{(32 - 22a^2 - 3a^4) E(k) - a^2(16 - 9a^2) K(k) -
$$

$$
- 2(1 - a^2\eta^2)^{3/2} (16 - 15a^2 + 24a^2\eta^2)\} \qquad \qquad \text{(IV.4)}
$$

$$
\frac{w^{(4)}}{c_1 KV} = \frac{8}{105a^6} \{(384 - 464a^2 + 124a^4 - 15a^6) E(k) - a^2(192 - 208a^2 + 45a^4) K(k) -
$$

$$
- 2(1 - a^2\eta^2)^{3/2} (192 - 280a^2 + 105a^4 + 12a^2\eta^2(24 - 35a^2) + 360a^4\eta^4)\}
$$

20

We now require the quantities

$$\varkappa^{(m,\,n)} = -\frac{4}{\pi} \int_0^1 \frac{l^{(m)}}{4K^2 c_1} \frac{w^{(n)}}{c_1 KV} \, d\eta$$

for $2 \leqslant m,\, n \leqslant 4$. We find, in terms of

$$I_n = \int_0^1 (1 - a^2\eta^2)^{3/2} (1 - \eta^2)^{1/2} \eta^{2n} \, d\eta$$

the following expressions :

$$\varkappa^{(2,\,2)} = \frac{128}{9\pi a^2} (2I_1 + I_0) - \frac{8}{3a^2} \{(2 - a^2)\, E(k) - a^2 K(k)\}$$

$$\varkappa^{(2,\,3)} = \frac{128}{45\pi a^4} \{48a^2 I_2 + (32 - 6a^2)I_1 + (16 - 15a^2)I_0\} -$$
$$- \frac{8}{15a^4} \{(32 - 22a^2 - 3a^4)\, E(k) - a^2(16 - 9a^2)\, K(k)\}$$

$$\varkappa^{(3,\,2)} = \frac{128}{15\pi a^2} (16I_2 - 2I_1 + I_0) - \frac{8}{3a^2} \{(2 - a^2)\, E(k) - a^2\, K(k)\}$$

$$\varkappa^{(3,\,3)} = \frac{128}{75\pi a^4} \{384a^2 I_3 + (256 - 288a^2)I_2 - (32 - 54a^2)I_1 + (16 - 15a^2)I_0\} -$$
$$- \frac{8}{15a^4} \{(32 - 22a^2 - 3a^4)\, E(k) - a^2(16 - 9a^2)\, K(k)\}$$

$$\varkappa^{(2,\,4)} = \frac{256}{315\pi a^6} \{720a^4 I_3 - (480a^4 - 576a^2)I_2 - (210a^4 + 272a^2 - 384)I_1 +$$
$$+ (105a^4 - 280a^2 + 192)I_0\} -$$
$$- \frac{16}{105a^6} \{(384 - 464a^2 + 124a^4 - 15a^6)\, E(k) - a^2(192 - 208a^2 + 45a^4)\, K(k)\}$$

$$\varkappa^{(4,\,2)} = \frac{256}{21\pi a^2} (48I_3 - 32I_2 + 4I_1 + I_0) - \frac{8}{3a^2} \{(2 - a^2)E(k) - a^2 K(k)\}$$

$$\varkappa^{(3,\,4)} = \frac{256}{525\pi a^6} \{5760a^4 I_4 - a^2(7440a^2 - 4608)I_3 + (2880a^4 - 5056a^2 + 3072)I_2 -$$
$$- (630a^4 - 848a^2 + 384)I_1 + (105a^4 - 280a^2 + 192)I_0\} -$$
$$- \frac{16}{105a^6} \{(384 - 464a^2 + 124a^4 - 15a^6)E(k) - a^2(192 - 208a^2 + 45a^4)K(k)\}$$

$$\varkappa^{(4,\,3)} = \frac{256}{105\pi a^4} \{1152a^2 I_4 + (768 - 1488a^2)I_3 + (576a^2 - 512)I_2 + (64 - 36a^2)I_1 +$$
$$+ (16 - 15a^2)I_0\} -$$
$$- \frac{8}{15a^4} \{(32 - 22a^2 - 3a^4)E(k) - a^2(16 - 9a^2)K(k)\}$$

$$\varkappa^{(4,\,4)} = \frac{512}{735\pi a^6} \{17280 I_5 - a^2(31680a^2 - 13824)I_4 + (19920a^4 - 22656a^2 + 9216)I_3 -$$
$$- (4680a^4 - 10112a^2 + 6144)I_2 - (832a^2 - 768)I_1 + (105a^4 - 280a^2 +$$
$$+ 192)I_0\} -$$
$$- \frac{16}{105a^6} \{(384 - 464a^2 + 124a^4 - 15a^6)E(k) - a^2(192 - 208a^2 + 45a^4)K(k)\}.$$

(IV.5)

21

The calculation of I_n as a function of a is described in Appendix V.

If now

$$l = \lambda l^{(2)} + \mu l^{(3)} + \nu l^{(4)} \quad .. \qquad .. \qquad .. \qquad .. \qquad .. \qquad .. \qquad .. \qquad .. \quad (IV.6)$$

then

$$w = \lambda w^{(2)} + \mu w^{(3)} + \nu w^{(4)} \qquad .. \qquad .. \qquad .. \qquad .. \qquad .. \qquad .. \qquad .. \quad (IV.7)$$

and

$$\varkappa = \frac{\pi A C_{Di}}{C_L{}^2} = \lambda^2 \varkappa^{(2,2)} + \lambda\mu\left(\varkappa^{(2,3)} + \varkappa^{(3,2)}\right) + \mu^2 \varkappa^{(3,3)} +$$
$$+ \nu\lambda\left(\varkappa^{(2,4)} + \varkappa^{(4,2)}\right) + \mu\nu\left(\varkappa^{(3,4)} + \varkappa^{(4,3)}\right) + \nu^2\varkappa^{(4,4)} . \quad .. \quad (IV.8)$$

$l^{(2)}$, $l^{(3)}$ and $l^{(4)}$ have the same integral from 0 to 1, so we require a minimum of $\varkappa$ subject to $\lambda + \mu + \nu = 1$. This leads to three simultaneous linear equations for λ, μ and ν which are solved for each value of a considered. With these values of λ, μ, ν, equations (IV.6) and (IV.7) give the optimum load distribution and upwash distribution for the value of a considered, using four terms only. The corresponding value of $\varkappa$ is given by (IV.8). This calculation has been taken as far as obtaining the value of $\varkappa$, but the load and upwash distributions have not been calculated. The same procedure has been followed using $l^{(2)}$ and $l^{(3)}$ only {$i.e.$, $\nu = 0$ in (IV.6) to (IV.8)}. This is considerably simpler and the optimum load and upwash distributions for $a = \sin 30$, 60 and 90 deg have been calculated and plotted in Figs. 8 and 9, using 3 terms only.

APPENDIX V

The Evaluation of Certain Complete Elliptic Integrals

Consider

$$J_n = \int_0^{\pi/2} \frac{\sin^{2n} x}{(1 - a^2 \sin^2 x)^{1/2}} \, dx \ .$$

Let $\sin x = \operatorname{sn}(a, u)$, then

$$J_n = \int_0^{\operatorname{sn}^{-1} 1} \operatorname{sn}^{2n} u \, du \ .$$

Now

$$\int \operatorname{sn}^{2n} u \, du = \frac{\operatorname{cn} u \, \operatorname{dn} u \, \operatorname{sn}^{2n-3} u}{(2n-1)a^2} + \frac{(2n-2)(1+a^2)}{(2n-1)a^2} \int \operatorname{sn}^{2(n-1)} u \, du -$$

$$- \frac{2n-3}{(2n-1)a^2} \int \operatorname{sn}^{2(n-2)} u \, du$$

as may be derived by differentiation. Hence

$$J_n = \{(2n-2)(1+a^2)J_{n-1} - (2n-3)J_{n-2}\}/(2n-1)a^2 \qquad \cdots \qquad \cdots \quad \text{(V.1)}$$

$$J_0 = K(a)$$

$$J_1 = \int_0^{\operatorname{sn}^{-1} 1} \operatorname{sn}^2 u \, du = \frac{1}{a^2} \int_0^{\operatorname{sn}^{-1} 1} (1 - \operatorname{dn}^2 u) \, du = \frac{1}{a^2} \{K(a) - E(a)\} \ .$$

From these three equations J_n may be calculated as a function of a, but the accuracy diminishes as n increases, rapidly if a is small.

Now consider

$$I_n = \int_0^1 (1 - a^2 \eta^2)^{3/2} (1 - \eta^2)^{1/2} \eta^{2n} \, d\eta \ .$$

Let $\eta = \operatorname{sn}(a, u)$. Then

$$I_n = \int_0^{\operatorname{sn}^{-1}} \operatorname{sn}^{2n} u \, \operatorname{cn}^2 u \, \operatorname{dn}^4 u \, du = J_n - (2a^2 + 1)J_{n+1} + a^2(2 + a^2)J_{n+2} - a^4 J_{n+3}$$

$$= \frac{2n + 9 - (2n+1)a^2}{(2n+3)(2n+5)} J_n + \frac{(2n+2)a^4 - (2n+7)a^2 - 3}{(2n+3)(2n+5)} J_{n+1} \cdot \quad \cdots \quad \text{(V.2)}$$

From this equation I_n may be calculated as a function of a from the values of J_n obtained.

APPENDIX VI

The Conically-Cambered Delta Wing for Small Values of $a = \tan \gamma / \tan \mu$

Equation (6) gives, on integration by parts,

$$\frac{w(\eta)}{c_1 KV} = \int_{1/a}^{\eta} \sqrt{(1 - a^2 \eta'^2)} \left\{ \frac{d}{d\eta'} \left(\frac{w(\eta')}{c_1 KV} \right) \right\}_{a=0} d\eta'$$

$$= \sqrt{(1 - a^2 \eta^2)} \left\{ \frac{w(\eta)}{c_1 KV} \right\}_{a=0} + a^2 \int_{1/a}^{\eta} \frac{\eta'}{\sqrt{(1 - a^2 \eta'^2)}} \left\{ \frac{w(\eta')}{c_1 KV} \right\}_{a=0} d\eta' \quad \text{(VI.1)}$$

If the load distribution is given by (11) or (I.12) as

$$\frac{l}{4K^2 c_1} = \frac{1}{\sin \psi} + \sum_2^{\infty} \frac{c_n}{c_1} \left(2n \sin(2n - 1)\psi + (2n - 1) \frac{\cos 2n\psi}{\sin \psi} \right) \quad \cdots \quad \cdots \quad \text{(VI.2)}$$

the corresponding upwash at $a = 0$ in the plane $z = 0$ is

$$\frac{w}{c_1 KV} = -1 - \sum_2^{\infty} \frac{c_n}{c_1} \frac{(2n - 1) \sin(2n - 1)\psi}{\sin \psi} \quad (\eta = \cos \psi, \text{ on the wing}) \cdots \text{(VI.3)}$$

and

$$\frac{w}{c_1 KV} = \sum_1^{\infty} \frac{c_n}{c_1} \frac{(2n - 1) e^{-(2n-1)\phi}}{\sinh \phi} \quad (\eta = \cosh \phi, \text{ off the wing}) \quad \cdots \quad \cdots \quad \text{(VI.4)}$$

by equation (I.4). The range of integration in (VI.1) extends from the Mach cone to the point of the wing and so both (VI.3) and (VI.4) are needed.

Consider first

$$\int_1^{\eta} \frac{\eta'}{\sqrt{(1 - a^2 \eta'^2)}} \left\{ \frac{w(\eta')}{c_1 KV} \right\}_{a=0} d\eta' = \int_0^{\psi} \cos \psi' \left(1 + \sum_2^{\infty} \frac{c_n}{c_1} \frac{(2n - 1) \sin (2n - 1)\psi'}{\sin \psi'} \right) \sin \psi' \, d\psi' + O(a^2)$$

$$= \frac{1}{4} \left[1 - \cos 2\psi + \sum_2^{\infty} \frac{c_n}{c_1} (2n - 1) \left(\frac{1 - \cos 2n\psi}{n} + \right. \right.$$

$$\left. \left. + \frac{1 - \cos (2n - 2)\psi}{n - 1} \right) \right] + O(a^2) \cdots \quad \cdots \quad \cdots \quad \cdots \quad \text{(VI.5)}$$

Now consider

$$\int_{1/a}^{1} \frac{\eta'}{\sqrt{(1 - a^2 \eta'^2)}} \left\{ \frac{w(\eta')}{c_1 KV} \right\}_{a=0} d\eta' = \int_{\bar{\phi}}^{0} \cosh \phi \sum_1^{\infty} \frac{c_n}{c_1} \frac{(2n - 1)e^{-(2n-1)\phi}}{\sinh \phi} \sinh \phi \, d\phi +$$

$$+ \sum_{r=1}^{\infty} \binom{-\frac{1}{2}}{r} (- a^2)^r \int_{\bar{\phi}}^{0} \cosh^{2r+1}\phi \sum_{n=1}^{\infty} \frac{c_n}{c_1} (2n - 1)e^{-(2n-1)\phi} \, d\phi$$

$$\cdots \quad \cdots \quad \text{(VI.6)}$$

where $\cosh \bar{\phi} = 1/a$ and uniform convergence is assumed. We have

$$\int_{\bar{\phi}}^{0} \cosh^{2r+1}\phi \, e^{-(2n-1)\phi} d\phi = - \frac{1 + O(a^2)}{2^{2n}(r - n + 1)a^{2(r-n+1)}} + O(1), \text{ since } e^{\bar{\phi}} = \frac{2}{a}\{1 + O(a^2)\}$$

and

$$\int_{\bar{\phi}}^{0} \cosh \phi \, e^{-(2n-1)\phi} \, d\phi = \begin{cases} \frac{1}{4}(e^{-2\bar{\phi}} - 1 - 2\bar{\phi}) & \text{if } n = 1 \\ \frac{1}{4}\left(\frac{e^{-2(n-1)\bar{\phi}} - 1}{n - 1} + \frac{e^{-2n\bar{\phi}} - 1}{n} \right) & \text{if } n > 1 . \end{cases}$$
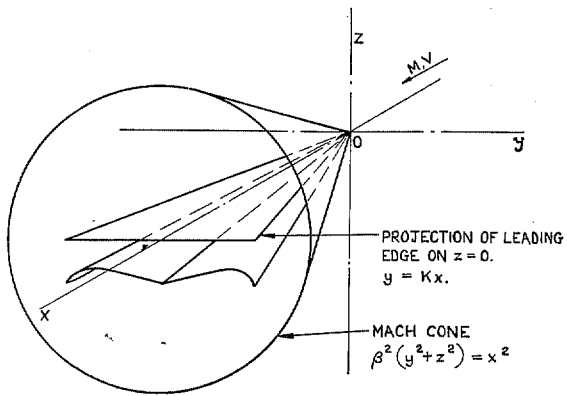
24

Thus (VI.6) becomes

$$\int_{1/a}^{1} \frac{\eta'}{\sqrt{(1 - a^2\eta'^2)}} \left\{ \frac{w(\eta')}{c_1 KV} \right\}_{a=0} d\eta' = -\tfrac{1}{4} \left\{ 2 \log \frac{2}{a} + 1 + 2 \log 2 + \sum_{2}^{\infty} \frac{c_n}{c_1} (2n - 1) \left(\frac{1}{n-1} + \frac{1}{n} \right) + \right.$$
$$\left. + O(a^2 \log a) . \qquad .. \qquad .. \qquad .. \qquad .. \qquad .. \qquad .. \text{(VI.7)} \right.$$

Lastly consider, for $|\eta| < 1$,

$$\sqrt{(1 - a^2\eta^2)} \left\{ \frac{w(\eta)}{c_1 KV} \right\}_{a=0} = -\left\{ 1 - \frac{a^2}{2} \cos^2\psi + O(a^4) \right\} \left\{ 1 + \sum_{2}^{\infty} \frac{c_n}{c_1} \frac{(2n-1) \sin (2n-1)\psi}{\sin \psi} \right\}$$

$$= -1 - \sum_{2}^{\infty} \frac{c_n}{c_1} \frac{(2n-1) \sin (2n-1)\psi}{\sin \psi} +$$

$$+ \frac{a^2}{4} \left\{ 1 + \cos 2\psi + 2 \sum_{2}^{\infty} \frac{c_n}{c_1} \frac{(2n-1) \sin (2n-1)\psi}{\sin \psi} + \right.$$

$$\left. + \sum_{2}^{\infty} \frac{c_n}{c_1} (2n-1) (\cos 2n\psi - \cos (2n-2)\psi) \right\} + O(a^4) \dots \text{(VI.8)}$$

Then, by using (VI.5), (VI.7) and (VI.8) in (VI.1), we have

$$\frac{w(\eta)}{c_1 KV} = -1 - \sum_{2}^{\infty} \frac{c_n}{c_1} (2n-1) \frac{\sin (2n-1)\psi}{\sin \psi} +$$

$$+ \frac{a^2}{4} \left\{ 1 - 2 \log \frac{4}{a} + \sum_{2}^{\infty} \frac{c_n}{c_1} (2n-1) \right\} \left\{ \frac{2 \sin (2n-1)\psi}{\sin \psi} + \frac{n-1}{n} \cos 2n\psi - \right.$$

$$\left. - \frac{n}{n-1} \cos (2n-2)\psi \right\} + O(a^4 \log a) . \qquad .. \qquad .. \qquad .. \qquad .. \qquad .. \text{(VI.9)}$$

The corresponding load distribution is (VI.2). Hence to calculate

$$\varkappa = \frac{\pi A C_{Di}}{C_L^2} = -\int_{0}^{1} \frac{l}{4K^2 c_1} \frac{w}{c_1 KV} d\eta$$

we require these simple integrals for positive (non-zero) integers m and n,

$$\int_{0}^{\pi/2} \sin(2m - 1)\psi \, \sin(2n - 1)\psi \, d\psi = \begin{cases} 0 & m \neq n \\ \pi/4 & m = n \end{cases}$$

$$\int_{0}^{\pi/2} \sin(2m - 1)\psi \, \cos 2n\psi \, \sin \psi \, d\psi = \begin{cases} 0 & m \neq n, n+1 \\ \pi/8 & m = n + 1 \\ -\pi/8 & m = n \end{cases}$$

$$\int_{0}^{\pi/2} \frac{\cos 2m\psi \, \sin(2n - 1)\psi \, d\psi}{\sin \psi} = \begin{cases} 0 & m \geqslant n \\ \pi/2 & m < n \end{cases}$$

$$\int_{0}^{\pi/2} \cos 2m\psi \, \cos 2n\psi \, d\psi = \begin{cases} 0 & m \neq n \\ \pi/4 & m = n . \end{cases}$$

25

Making use of these and remembering

$$\sum_{2}^{\infty} \frac{c_n}{c_1} (2n - 1) = -1 \qquad \cdots \qquad \cdots \qquad \cdots \qquad \cdots \qquad \cdots \qquad \cdots \qquad \cdots \qquad ..(\text{VI.10})$$

since the load vanishes at $\psi = 0$, we find, neglecting $O(a^4 \log a)$,

$$\varkappa = 1 + \sum_{2}^{\infty} \left(\frac{c_n}{c_1}\right)^2 (2n - 1) + a^2 \log \frac{4}{a} +$$

$$+ \frac{a^2}{4} \sum_{2}^{\infty} \left\{ \left(\frac{c_n}{c_1}\right)^2 \frac{(2n-1)(n^2 - n + 1)}{n(n-1)} + \frac{c_n \, c_{n+1}}{c_1^2} \frac{2(n^2 - 1)}{n} \right\}. \qquad (\text{VI.11})$$

We now seek to minimize $\varkappa$, subject to (VI.10), considering first the case $c_n/c_1 = 0$ for $n > N$. Since $\varkappa$ is given by (VI.11) only to the first order in a^2, we write

$$\frac{c_n}{c_1} = -\frac{1}{N^2 - 1} + a^2 \varepsilon_n, \qquad n \leqslant N \, ,$$

since this tends to the slender-wing optimum as $a \to 0$. Substituting this in (VI.11) and (VI.10), neglecting terms in $\varkappa$ independent of ε_n, we find that the problem is to minimize

$$\frac{\varepsilon_N}{2N} + \sum_{2}^{N} (2n - 1) \, \varepsilon_n^2 \quad \text{subject to} \quad \sum_{2}^{N} (2n - 1) \, \varepsilon_n = 0.$$

The usual procedure of the undetermined multiplier leads to

$$\varepsilon_n = \frac{1}{4N(N^2 - 1)} \quad 2 \leqslant n < N$$

$$\varepsilon_N = -\frac{N - 2}{4(N^2 - 1)(2N - 1)}$$

and so to

$$\frac{c_n}{c_1} = -\frac{1}{N^2 - 1} \left(1 - \frac{a^2}{4N}\right) \quad 2 \leqslant n < N$$

and

$$\frac{c_N}{c_1} = -\frac{1}{N^2 - 1} \left(1 + \frac{(N-2)a^2}{4(2N-1)}\right).$$

The corresponding value of $\varkappa$ becomes, after reduction,

$$\varkappa_N = 1 + \frac{1}{N^2 - 1} + a^2 \log \frac{4}{a} + \frac{(2N - 1)}{N(N^2 - 1)} \frac{a^2}{4}. \qquad \cdots \qquad \cdots \qquad ..(\text{VI.12})$$

As $a \to 0$, $\varkappa_N \to 1 + 1/(N^2 - 1)$, the slender-wing value.

As $N \to \infty$, $\varkappa_N \to 1 + a^2 \log (4/a)$, the first terms of the value for the flat plate viz., $\varkappa = 2E(k) - k$, $k^2 = 1 - a^2$.

26

FIG. 1.   Co-ordinate system, wing and Mach cone.
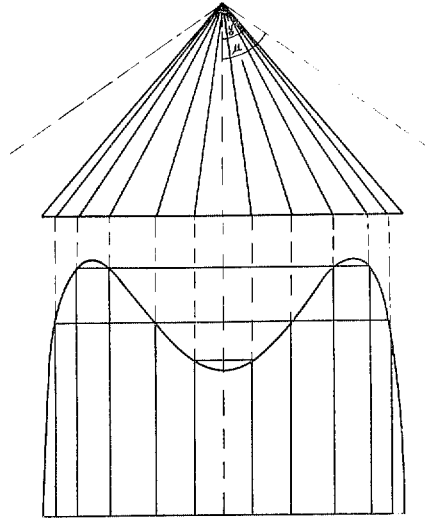
FIG. 2.   Composition of a conical load distribution from constant incremental loads.
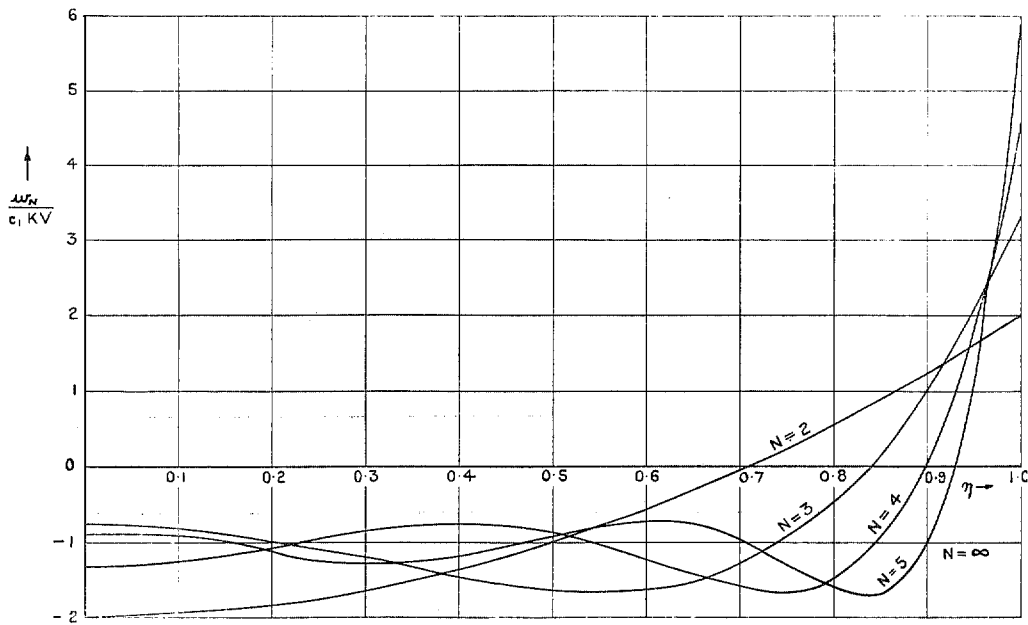
FIG. 3.   Optimum upwash distributions for slender wings. $(a = 0)$, $N = 2, 3, 4, 5.$
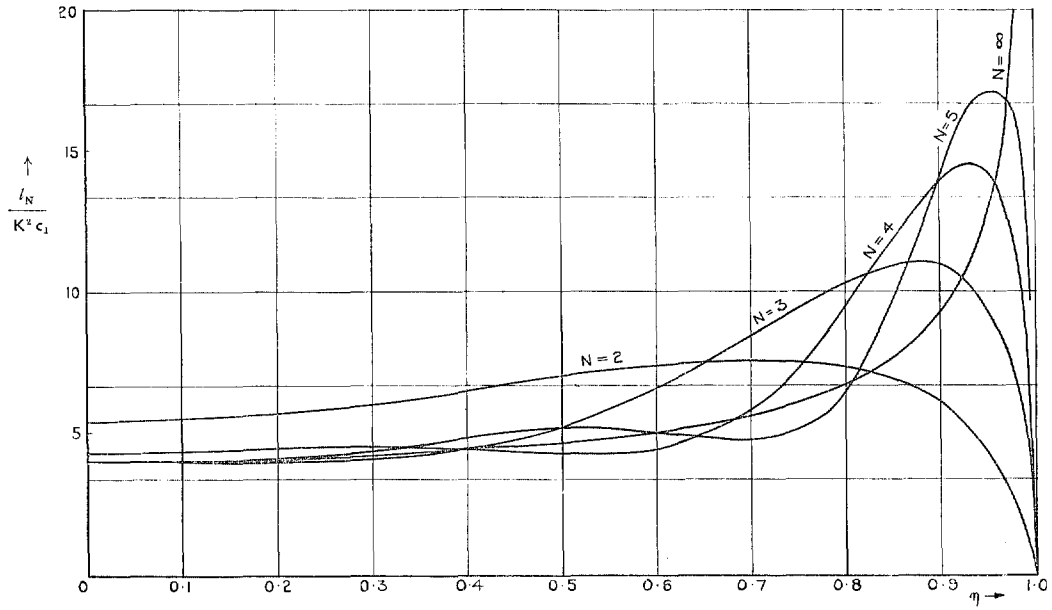
FIG. 4. Optimum load distributions for slender wings. $(a = 0)$, $N = 2, 3, 4, 5$.
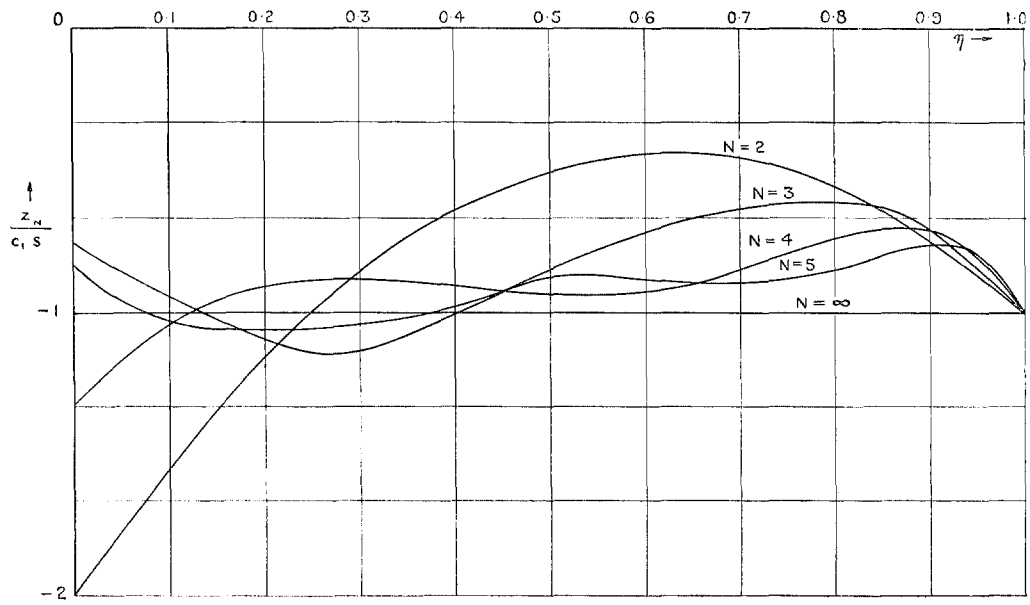
FIG. 5. Optimum cross-sections for slender wings. $(a = 0)$, $N = 2, 3, 4, 5$.

28
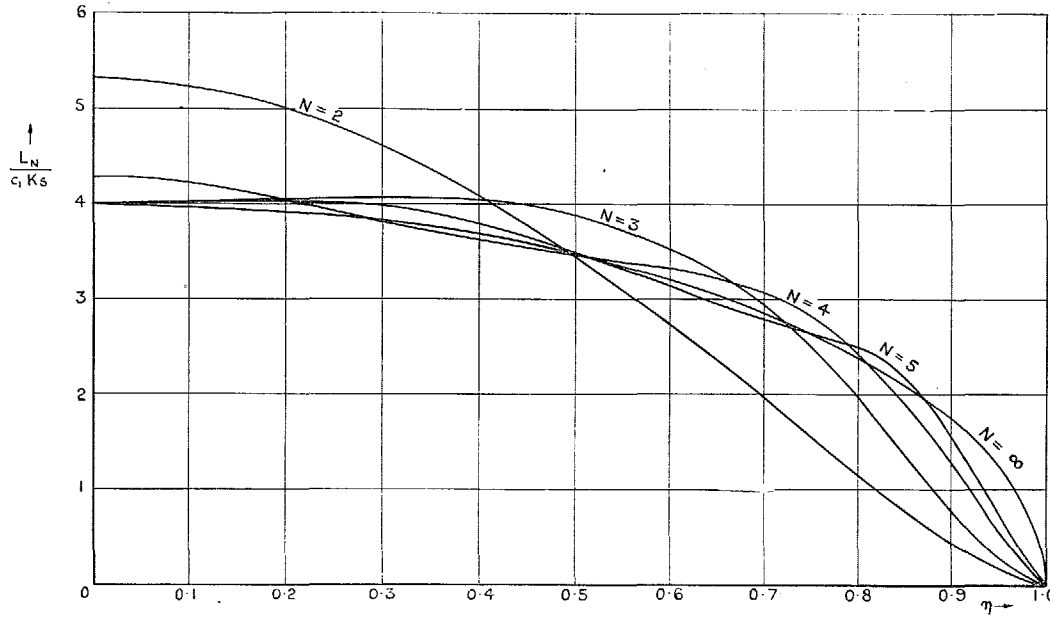
FIG. 6. Spanwise distribution of chord loading for optimum slender wings.
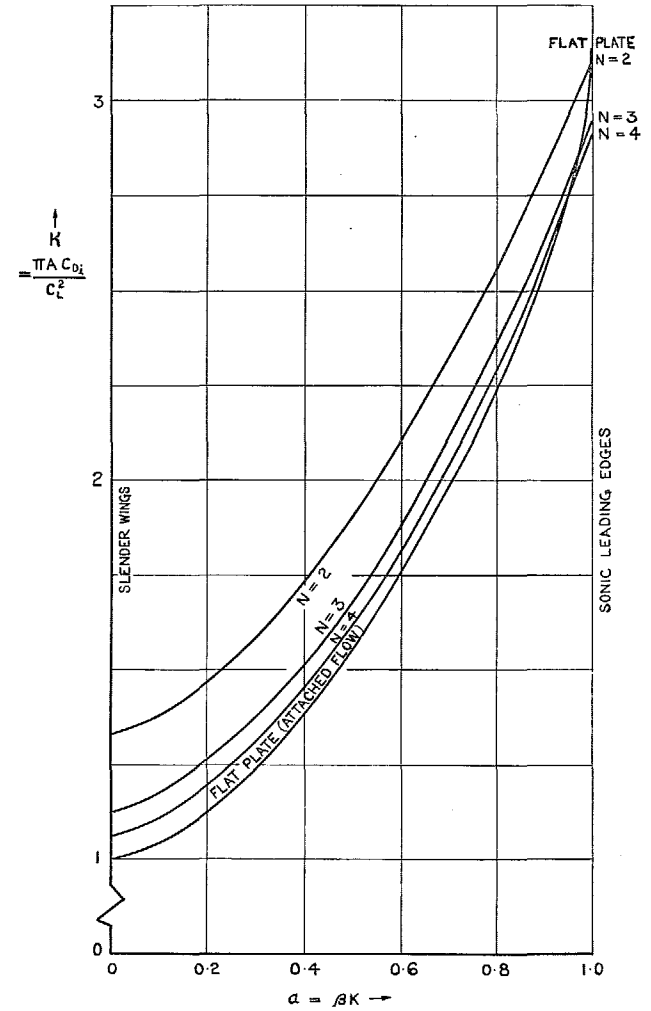
FIG. 7. Lift-dependent drag factor for conically-cambered wings using 2, 3, and 4 terms.
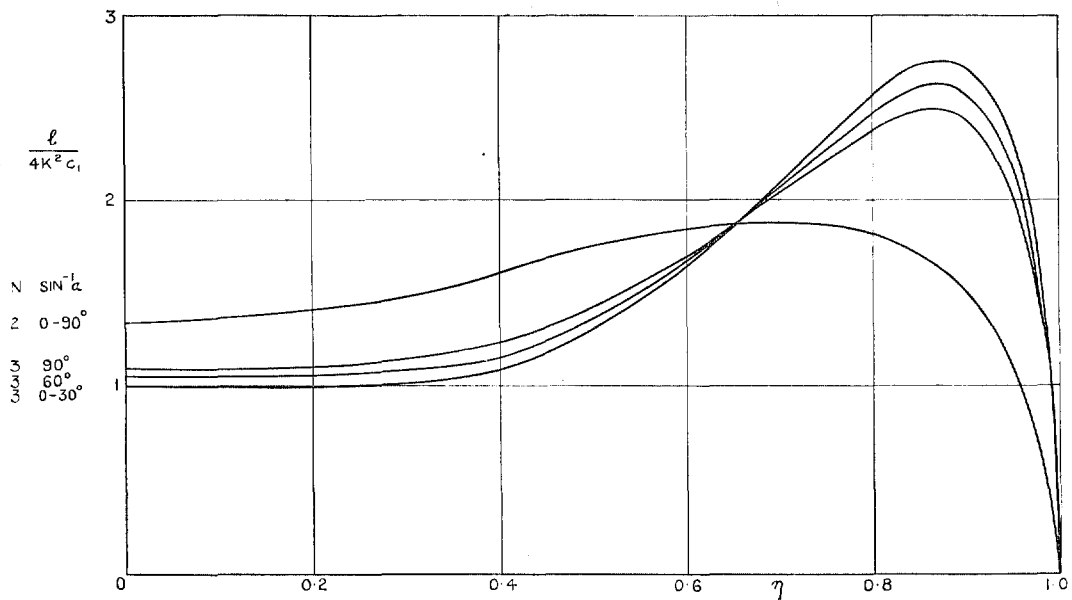
Fig. 8.   Optimum load distributions across the span for $N = 2, 3$; $0 \leqslant a \leqslant 1$.
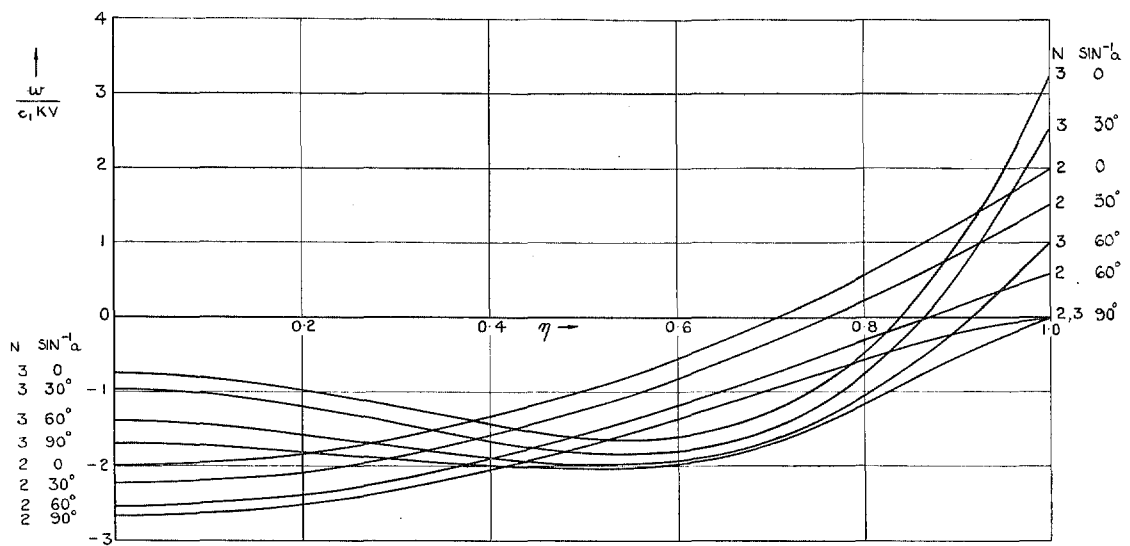
Fig. 9.   Optimum upwash distributions across the span for $N = 2, 3$; $0 \leqslant a \leqslant 1$.

30
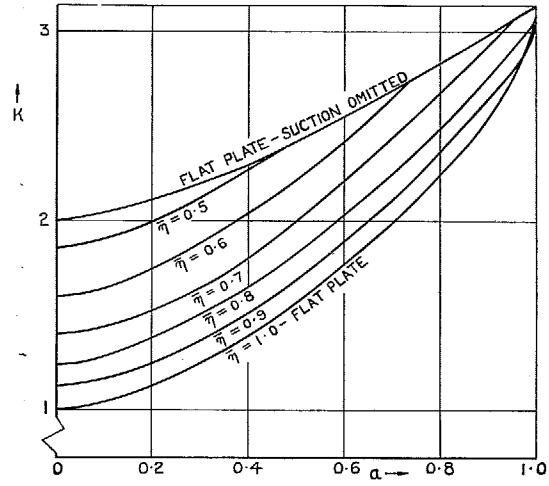
FIG. 10. Lift-dependent drag factor against
$a = \beta K$ for wings with flaps.
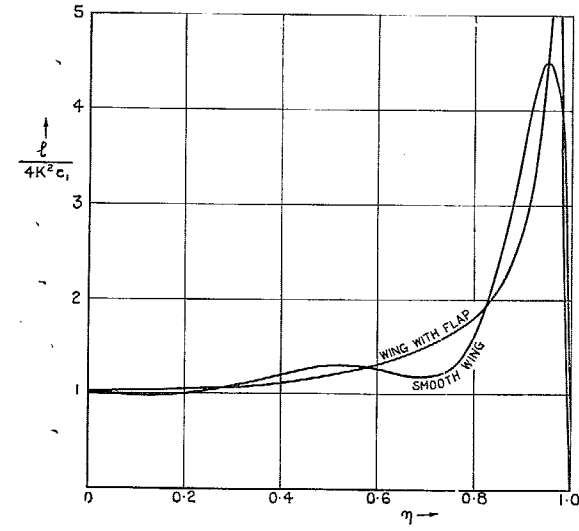
FIG. 12. Load distributions on smooth
$(N = 5)$ and kinked $(\bar{\eta} = 0 \cdot 966)$ slender
wings.

31
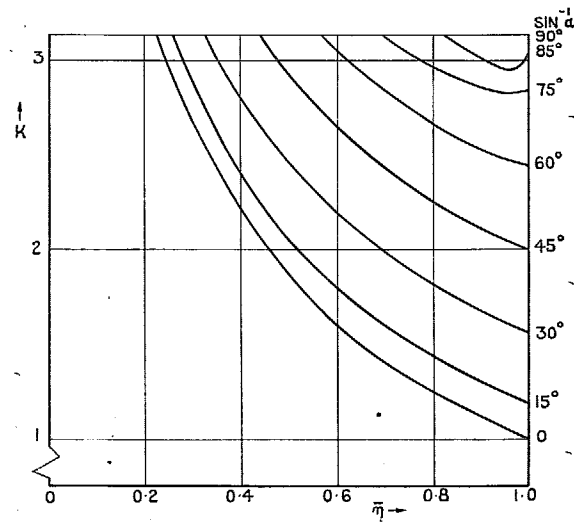
FIG. 11. Lift-dependent drag factor against
hinge position for wings with flaps.
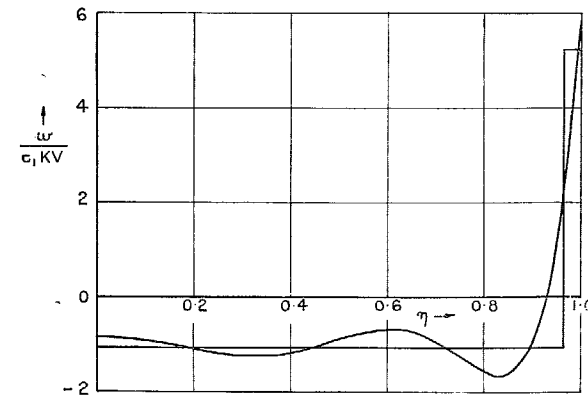
FIG. 13. Upwash distributions on smooth
$(N = 5)$ and kinked $(\bar{\eta} = 0 \cdot 966)$ slender
wings.
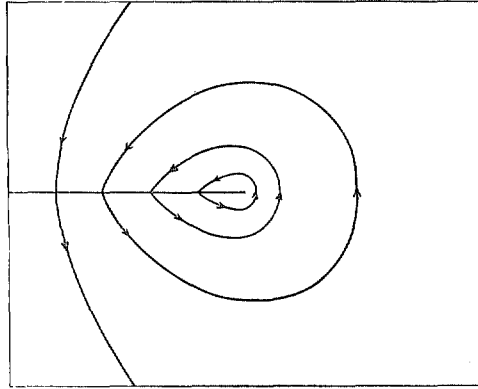
(a) FLAT PLATE
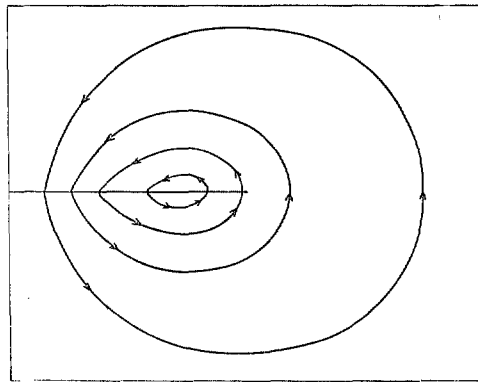
(b) CAMBERED PLATE.

FIG. 14a and b.   Approximate streamline
pattern of cross-flow for slender wings
(relative to stream).

Publications of the
Aeronautical Research Council

ANNUAL TECHNICAL REPORTS OF THE AERONAUTICAL RESEARCH COUNCIL (BOUND VOLUMES)

Annual Reports of the Aeronautical Research Council—

Index to all Reports and Memoranda published in the Annual Technical Reports, and separately—

Published Reports and Memoranda of the Aeronautical Research Council—

HER MAJESTY'S STATIONERY OFFICE